Regulation of vascular inflammation by selectin antagonists and transcription factor GATA5

Mathieu Joyal

A thesis Submitted to the University of Ottawa

In Partial Fulfilment of the Requirements for the

MSc degree in Biochemistry

Department of Biochemistry, Immunology and Microbiology

Faculty of Medicine

University of Ottawa

Abstract

Chronic inflammation is a complex immune response linked to several diseases. The first step in the inflammatory response is the recruitment of immune cells to the endothelium of the vascular wall. This process is mediated by E/P-Selectin, for which no antagonist efficiently interacts to limit the inflammatory response. Previous work identified transcription factor GATA5 as a key regulator of endothelial homeostasis and revealed an altered expression of inflammatory genes in human endothelial cells with loss of GATA5. The objective of my project is to understand the role of GATA5 in selectin-dependent vascular inflammation and to develop selectin inhibitors. I used biochemical, cellular and *in vivo* approaches to evaluate a series of novel small molecules for their ability to interfere with selectin binding to their ligand, PSGL-1. The work identified a new lead candidate, LCB 2248, for the development of new E/P-Selectin antagonists and contributed to the understanding of the role of GATA5 in cell recruitment and adhesion. The mechanistic insight gathered and the identification of an E/P-Selectin antagonist will hopefully pave the way for the development of effective treatments for patients with chronic inflammation.

Acknowledgements

First, I would like to thank Dr. Mona Nemer for accepting me in such a wonderful lab. Her guidance, knowledge were a great source of inspiration and motivation. Thank you for trusting me with the development of these new assays for our lab. Your passion for research is inspiring.

I would also like to thank our collaborators in the Guindon lab, Ryan Simard and Dr. Michel Prevost for synthesizing all these wonderful compounds that I had the pleasure of working with. My special thanks to Dr. Yvan Guindon for all his help and guidance and encouragement throughout my masters.

I am also very thankful to Drs Katey Rayner and Subash Sad for their inputs and suggestions. Their knowledge and guidance were instrumental to the success of this project.

A special thanks to my friend Dr. Wael Maharsy, my partner in crime in this project for all his knowledge, guidance, advice, and support to help me achieve my project goals.

I am also thankful for all the past and present members of the Nemer lab. Thanks for being great colleagues. My gratitude goes to Dr. Hiba Komati, Dr. Jamie Whitcomb, Dr. Lara Gharibeh, Laura Collins, Dr. Massy Sh-Hassani, Dr. Alice Lau, Dr. Yuejen Xju, Dr. Georges Kanaan, Dr. Omar Mansour, Justen Choueiry and Abir Almazloum. My special admiration and recognition to our lab technicians Janie Beauregard and Megan Fortier who always ensure we can perform our experiments and are always willing to help us obtain better results. I wish you all the best of luck in all your future endeavors.

Finally, my deepest thanks to my parents and family who've always supported and encouraged me.

Statement of Contributions

Surface plasmon resonance acquisition was performed by Mathieu. SPR data analysis was performed by Ryan Simard in Dr Guindon's laboratory. Selectin protein production and purification were performed by Janie Beauregard from Dr Nemer's laboratory. Cell-Selectin, Cell-Cell and peritoneal lavage experiments were performed by Mathieu. Original genome wide transcript data of GATA5 knockdown in human dermal microvascular endothelial cells was performed by Dr Smail Messaoudi. Further analysis of the microarray data was performed by Mathieu. Generation of GATA5 KD HDMECs was performed by Dr Smail Messaoudi and Mathieu. Generation of GATA5 overexpression HDMECs was performed by Mathieu. Evaluation of GATA5 levels in various endothelial cells was performed by Dr Smail Messaoudi. All other experiments including Primary lung endothelial cell isolation, QPCRs and western blots were performed by Mathieu.

Table of Contents

List of Abbreviations

AA Arachidonic acid

ABCA1 ATP-binding cassette sub-family A member 1

AMPKα2 5'-AMP-activated protein kinase catalytic subunit alpha-2

ARDS Acute respiratory distress

BAV Bicuspid aortic valve

BIRC5 Survivin

CAMs Cellular adhesion molecules

CD11b Cluster of differentiation molecule 11b

CD11c Integrin alpha-X

CLDN1 Claudin 1

CLDN2 Claudin 2

Clu Clusterin

COPD Chronic obstructive pulmonary disease

COX1 Cyclooxygenase 1

COX2 Cyclooxygenase 2

CXCR4 C-X-C chemokine receptor type 4

DAMPs Damage-associated molecular patterns

DMSO Dimethyl sulfoxide

DVT Deep vein thrombosis

ECM extracellular matrix

EGF Epidermal growth factor

ESL-1 E-selectin ligand 1

fuc Fucose

Gal Galactose

GlcNAc N-acetyl glucosamine

GLG-1 Golgi glycoprotein 1

HBB Beta globulin

HCAEC Human coronary artery endothelial cell

HCMEC Human cardiac microvascular endothelial cell

HDMEC Human dermal microvascular endothelial cells

HL-60 Human leukocyte like cells

HPMEC Human pulmonary microvascular endothelial cell

IC50 half maximal inhibitory concentration

ICAM1 Intercellular adhesion molecule 1

IL-1 Interleukin 1

IL-10 Interleukine 10

IL1A Interleukin 1 alpha

IL-6 Interleukin 6

IRCM Institut de recherche clinique de Montréal

ITGB8 Integrin beta 8

KD Knockdown

LFA-1 Lymphocyte function-associated antigen 1

Ly-6C Lymphocyte antigen 6 complex

Ly-6G Lymphocyte antigen 6G

Mac-1 Macrophage-1 antigen

mRNA messenger ribonucleic acid

Myh10 Myosin heavy chain 10

MYL9 Myosin light chain 9

NADPH Nicotinamide adenine dinucleotide phosphate

NeuAc N-acetylneuraminic acid

NF-ATc Nucelar factor of activated T cells 1

NFκB Nuclear factor-kappaB

NK Natural killer cells

NSAID Nonsteroidal anti-inflammatory drug

OCLN Occludin 1

Ovr Overexpression

PAMPs Pathogen-associated pattern molecules

PE Pulmonary embolism

PECAM1 Platelet and endothelial cell adhesion molecule 1

PGH2 Prostaglandin H2

PGG2 Prostaglandin G2

PKA Protein kinase A

PLA2 Phospholipase A2

PLAT Plasminogen activator, Tissue type

PRKCI Protein kinae c iota

PSGL-1 P-selectin glycoprotein ligand 1

S16 40S ribosomal protein S16

SEM Standard error mean

shRNA Short hair RNA

sLea Sialyl Lewis A

sLex Sialyl Lewis x

SPHK1 Sphingosine kinase 1

SPL1 Squamosa promoter-binding-like protein 1

SPR Surface plasmon resonance

QPCR Quantitative polymerase chain reaction

RNA ribonucleic acid

TJP1 Tight junction protein 1

TNF Tumor necrosis factor

TNFα Tumor necrosis factor alpha

TNFRSF1B Tumor necrosis factor receptor subfamily 1 beta

VCAM1 Vascular cell adhesion molecule 1

VTE venous thromboembolism

VWF von Willebrand factor

List of Tables

List of Figures

Introduction

1. Inflammation

Living organisms have developed a process known as inflammation, which is a response to the presence of a harmful stimulus, like the one caused by the invasion of a pathogen (virus, fungus, or parasite). There are two types of inflammatory responses triggered by the innate and adaptive immune systems[1]. Their goal is to allow the recruitment and activation of immune cells to the injury site. The adaptive response involves T and B cells that produce antibodies and usually, take several days to establish[2]. The innate response is fast, within minutes, and is initiated once a pathogen is introduced inside the organism[3]. The innate response includes macrophages, monocytes, natural killer (NK) cells, and dendritic cells. These responses lead to an increase in vascular leaking and cellular recruitment to the site of the injury, causing swelling.

1.1. Acute inflammatory response

The inflammatory response, characterised as acute or chronic, leads to the elimination of pathogens and cellular debris from damaged or dead cells. Immune cells that are implicated in the innate response ultimately recognise molecular motifs specific to pathogens, known as pathogen-associated pattern molecules (PAMPs)[4]. Macrophages, dendritic cells, and neutrophils eliminate the debris and pathogens using phagocytosis[5]. Phagocytosis is the process in which the cells "eat" and digest the debris and bacteria. During phagocytosis the immune cells, such as macrophages, surround the bacteria (or debris) with their cellular membrane forming a vacuole that then fuses with the lysosomes in the cells[6]. Lysosomes are organelles inside cells that contain several digestive enzymes in an acidic solution that degrades pathogens and debris[7]. Natural killer cells

eliminate damaged, infected, or altered cells. NK cells secrete cytotoxic mediators (perforin and granzymes), killing the altered cells[8]. They also release several pro-inflammatory cytokines, interleukins, interferons, and tumor necrosis factors (such as IL-6, INF1, and TNFα)[9]. Cytokines activate macrophages and guide their response to the inflamed area through chemotaxis[10]. The inflammatory response must be quick in order to protect the host but must not cause tissue damage or inhibit the function of the organism. The response is occasionally too strong becoming dangerous for the host.

An example of acute vascular inflammation is the venous thromboembolisms (VTE). VTE is estimated to affect 900 000 people in the United-States every year and causes 300 000 deaths, resulting in a 33% mortality rate[11]. VTE is the combination of deep vein thrombosis (DVT) and pulmonary embolism (PE). Deep vein thrombosis is the formation of a blood clot, known as thrombus, in the veins, usually, they are formed in the legs. These clots can dislodge and cause a pulmonary embolism[12]. The current treatment for DVT is anticoagulants[13]. However, anticoagulants are not able to break the thrombus and increase bleeding risks. They are also unable to prevent the development of post-thrombotic syndrome such as, leg pain, swelling, and venous ulcers[14]. The risks associated with the anticoagulants, led to the investigations of other treatments. Recently P-selectin, discussed further, and von Willebrand factor (VWF) have been associated with DVT. P-selectin and VWF promote the accumulation of platelets and leukocytes that promote injury on the vein wall and the formation of a thrombus[11,15].

1.2. Chronic inflammation

A prolonged inflammatory response can also have a negative effect on the organism. There are several different causes of chronic inflammation. One of the causes of chronic inflammation is a persistent infections or non-healed injuries leaving the host vulnerable to another pathogenic invasion. Chronic inflammation also has non-infectious causes such as diabetes and obesity. It has been found that adipocytes surrounding organs secrete pro-inflammatory cytokines such as TNFα and IL-6[16]. These usually cause damage to tissues leading to the release of damage-associated molecular patterns (DAMPS)[17]. DAMPS induce the secretion of inflammatory cytokines stimulating further the inflammatory response[18]. Until the cause of the tissue damage is removed or resolved the inflammatory stimulus persists[2]. Several diseases have been found to cause tissue damage that leads to chronic inflammation such as auto-immune diseases (rheumatoid arthritis), various cardiovascular diseases (hypertension and hypercholesterolemia), atherosclerosis, and tumors[19,20].

Chronic inflammation was previously treated with nonsteroidal anti-inflammatory drugs (NSAIDs)[21]. Some common NSAIDs are Ibuprofen, Aspirin, Tramadol, and Paracetamol. NSAIDs have been demonstrated to be effective against numeral diseases such as osteoarthritis, and rheumatoid arthritis[22]. They lower the levels of prostaglandins (ex. PGG2 and PGH2), which are part of the arachidonic acid derived eicosanoids by inhibiting cyclooxygenase enzymes (COX-1 and COX-2)[23]. Their biological response includes vascular homeostasis and platelet aggregation. NSAIDs are effective to reduce pain and inflammation but are however associated with several adverse side effects such as alterations in renal functions, hepatic injury, and platelet inhibition,

by blocking their ability to aggregate in a thromboxane dependant manner[24]. The most important adverse side effects are gastro-intestinal, these include an increase in the formation of ulcers, gastrointestinal hemorrhage, and perforation[25–27]. This led to the development of more specific inhibitors of COX2. Unfortunately, some of these inhibitors can cause cardiovascular toxicity[28].

Currently, inflammation is treated with corticosteroids. The biosynthesis of eicosanoids depends on the availability of free arachidonic acid (AA) which is produced from membrane phospholipids by the action of phospholipase A2 (PLA2). AA could then be converted to prostaglandins or leukotrienes, by cyclooxygenase and lipoxygenase, mediators of inflammation. Corticosteroids inhibit PLA2. Corticosteroids also suppress the inflammatory response by downregulating several pro-inflammatory genes that encode the production of chemokines, cytokines, and adhesion molecules[29]. At high doses they can also activate certain anti-inflammatory genes these include interleukin 10 (IL-10), annexin-1, and squamosa promoter-binding-like protein 1 (SPL1)[30]. Corticosteroids also inhibit the vasodilatation and increase in vascular permeability in the initial steps of inflammation[31]. While corticosteroids are very effective against certain inflammatory diseases, like asthma, they are not effective against all inflammatory diseases such as chronic obstructive pulmonary disease[32]. Corticosteroids can also cause adverse side effects. In short-term use, certain side effects can be observed such as truncal obesity, acne, hyperpigmentation, myopathy, hyperglycemia, and intracranial hypertension[33]. These adverse reactions are fortunately rare, and most of these effects will disappear after the steroid treatment. In long term corticosteroid use, the adverse reactions are more frequent and important. Long term treatments have been linked with the development of osteopenia, adrenal insufficiency, growth suppression, and congenital malformations[33–35].

2. Cellular and molecular basis of vascular inflammation

Inflammation involves changes to both the immune cells and the endothelial cells of the vascular wall. Once stimulated the endothelial cells will increase the expression of adhesion molecules. These adhesion molecules allow better recruitment of immune cells on the vascular wall. Stimulated immune cells will also increase the expression of the cellular adhesion ligands. The stimulation of the endothelial cells induces also an increase in vascular permeability[36]. In this work, we will focus on the response of endothelial cells in vascular recruitment.

2.1. Endothelial cell response and cell-cell interactions

Upon an inflammatory stimulus, damaged cells release cytokines such as tumor necrosis factor α (TNFα) and interleukin 1 (IL-1)[1]. These chemokines diffuse towards the endothelial cells of blood vessels to engage the immune cell recruitment which is spatially and timely controlled[37]. Upon stimulation, endothelial cells mobilise the selectins and other cellular adhesion molecules (CAMs) to their surface[38]. These cellular adhesion molecules are expressed at varying time periods after the presence of the stimulus. As describe further the presence of P-selectin at the cell surface is almost immediate while the expression of E-selectin can only be found three hours after the stimulus[39]. Selectins mediate the first step required for the migration of leukocytes from the bloodstream, the rolling and tethering of leukocytes in flow[40]. The "mechano chemistry" of selectin binding to its ligands on the leukocytes is complex. The K_{off} of the selectin ligands bound decreases when the force of the shear stress increases in the vessel. It reaches a minimum which means a longer interaction between the cell wall and the leukocytes. A further increase in shear stress will eventually lead to an increase in K_{off}. This modulation of the K_{off} under flow, has been

rationalized by conformational change of selectins and of their ligands under flow[41]. Interestingly shear stress to the vascular wall is influenced by flow and the size of the vessel, which in turn influences the adhesion of the vessels[42]. The role of the selectins is to induce the rolling of leukocytes which will eventually be immobilized by binding with high affinity to integrins, such as intercellular adhesion molecule 1 (ICAM1), binding the lymphocyte function-associated antigen 1 (LFA-1). Eventually, the extravasation and migration of the leukocyte to the inflamed site will be successfull[43] (Figure 1). The binding of the leukocytes to the vascular P-Selectin also increases their binding property to the interaction between the leukocytes and the selectins causes a conformational change to the LFA-1 ligand[44]. The ligand can adopt two conformations: a closed headpiece and an extended form with an open headpiece[44]. In the closed configuration, the ligands have a low affinity to the integrins. While in the open configuration the ligands have a high affinity and a longer bonding time for integrins. The interaction with the selectins triggers the extension of the closed headpiece to an open headpiece (Figure 2)[45]. The role of selectins is central to the vascular recruitment response as they are the first and rate-limiting step of the adhesion and extravasation of leukocytes to the inflamed site[46].

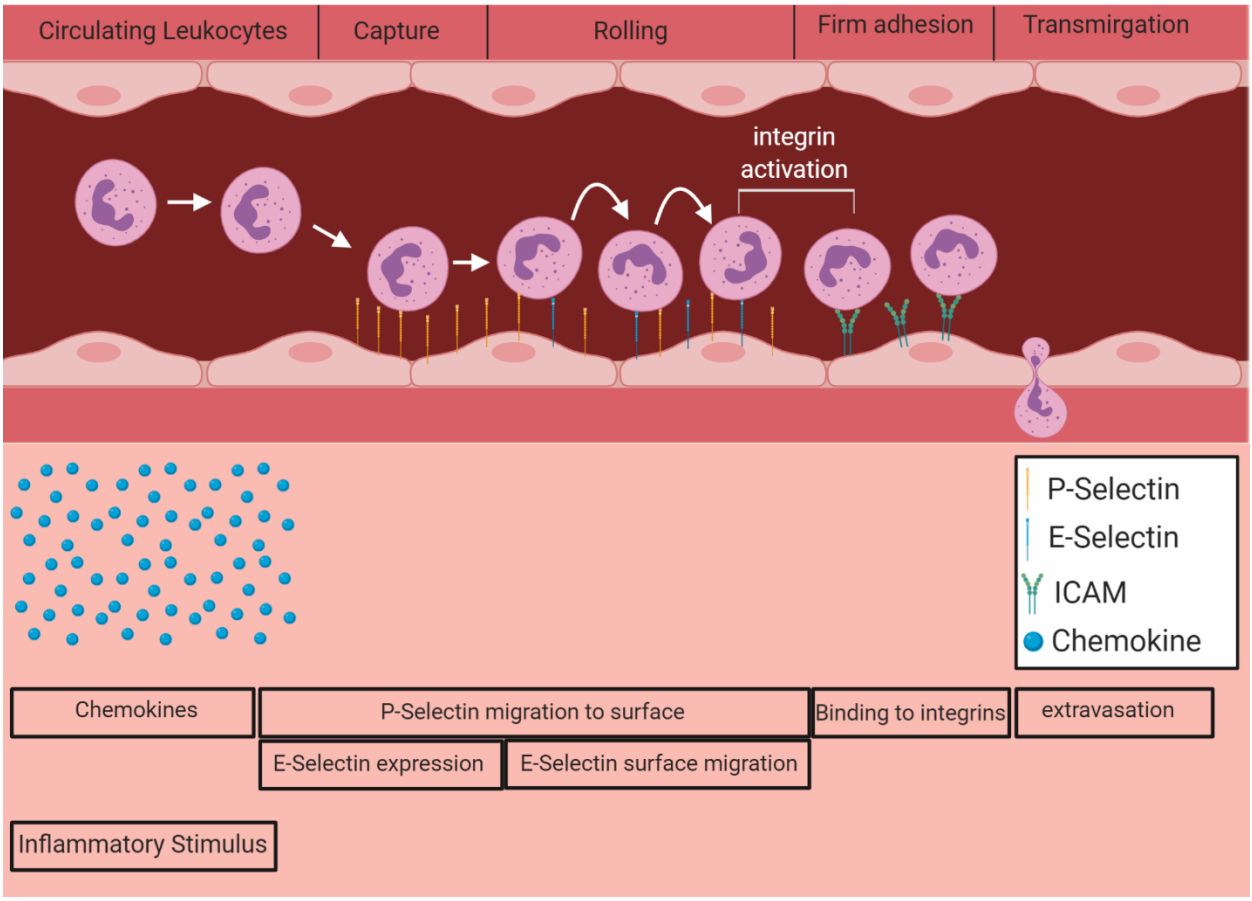

Figure 1. Schematic representation of vascular cell adhesion

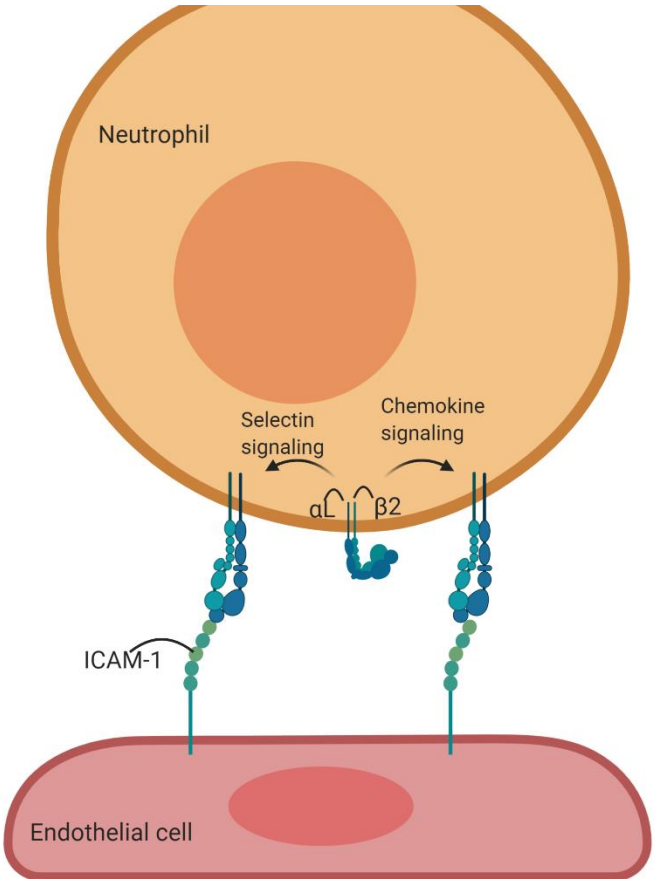

Figure 2. Schematic of LFA-1 and ICAM1 interaction in response to selectin and chemokine signaling. Created with biorender.com

2.2. Transcriptional regulation of inflammation

The inflammatory response is coordinated by the activation of several pathways, by the various cytokines, in leukocytes and in the endothelial cells. For example, the nuclear factor-kappaB (NFκB) pathway is considered a typical pro-inflammatory response. NFκB is known to activate multiple inflammatory genes these including P-selectin, IL-1, and IL-6[47]. Unfortunately, not all pro-inflammatory pathways and mechanisms have been identified. In this project, I will evaluate the potential role of the transcription factor GATA5 in the regulation of the inflammatory response in endothelial cells.

2.2.1. Endothelial cell homeostasis

Disruptions in the vascular functions have been associated with the development of several diseases including, atherosclerosis, sepsis, and cancer[48]. These disruptions cause improper vascular homeostasis. One of the important players in the communication between the vessels and the outer microenvironment are the endothelial cells. Endothelial cells often respond to the extracellular signals which lead to the spatial and temporal regulation of various gene expression. The mechanisms involved in the regulation of endothelial cell-specific genes are currently under active investigation. One of the earliest identified regulators of endothelial homeostasis is the transcription factor GATA2[49]. In humans, the family of GATA transcription factors is comprised of six members that bind to the WGATAR motif on promoters of genes they regulate[50,51]. GATA factors 1,2 and 3 are mainly found in hematopoietic cells and in the nervous system. GATA 2 is also expressed in all endothelial cells[52]. In endothelial cells, GATA2 has been found to activate the expression of endothelin 1, platelet/endothelial cell adhesion molecule 1 (PECAM1), von Willebrand factor, and vascular endothelial cells adhesion molecule 1[49]. GATA factors 4, 5, and 6 are predominantly expressed in the heart and in cells of the digestive tract.[51]. Recently our lab has discovered that GATA5 is enriched in the endocardium and in some vascular endothelial cells. also plays a key role in the regulation of endothelial cell homeostasis.

2.2.2. GATA5

GATA5 is expressed in multiple tissues: liver, kidney, lungs, intestines, and the heart. In the heart, GATA5 expression can only be observed in endothelial derived cells. It has been shown that GATA5 and NF-ATc synergistically activate the endocardial transcription. This study revealed

that the expression of GATA5 is required for terminal differentiation of cardiac progenitor endothelial cells[53]. Its role in the differentiation of endothelial cells was then evaluated in the septation and formation of the cardiac valves. In our lab using Gata5 null mice, we discovered that the loss of Gata5 lead to the development of a bicuspid aortic valve (BAV)[54]. Further work from our group has revealed that the mice lacking GATA5 are hypertensive likely due to vascular causes The role of GATA5 in endothelial homeostasis was further supported by the finding that variants in the human *GATA5* gene are linked to high blood pressure[55]. As mentioned above, several cardiovascular diseases lead to chronic inflammation and in turn, vascular inflammation can lead to cardiovascular complications including hypertension, atherosclerosis, and heart failure. Thus, GATA5 may be an important player in endothelial homeostasis and the inflammatory response. Consistent with this, human dermal microvascular endothelial cells (HDMECs), with knocked down GATA5 expression using short hair RNA (shRNA), show increased levels of several pro-inflammatory genes, such as ICAM1 and IL-6[55]. Expression of two homeostasis associated kinases, protein kinase A (PKA) and 5'-AMP-activated protein kinase catalytic subunit alpha-2 (AMPKα2), was also decreased in the knockdown cells. PKA and AMPKα2 are known to be implicated in the control of inflammation through among of them, the regulation of NAPDH oxidase[56,57]. We, therefore, hypothesise that our Gata5 null mice could be a novel inflammatory model.

3. Selectin dependant migration in inflammation

3.1. Members of the selectin family

Selectins are cell adhesion molecules and are the main mediators in the initial steps of leukocyte recruitment in response to an inflammatory stimulus[58]. There are three different selectins E, P, and L. They are all composed of the same elements: a C-type lectin domain, an epidermal growth factor (EGF)-like domain, and a complement regulatory domain[59]. The structural difference between them is the number of repeats of the complement regulatory domain (Figure 3). Selectin binding is calcium dependent[60]. Both E and P selectins are expressed on the surface of blood vessels while L-selectin is expressed on the surface of immune cells. P-selectin can also be found on the surface of platelets[61–63]. In this work, we focus on the interaction of E and P at the surface of blood vessels. P-selectin is kept in stock in the Weibel-Palade bodies until it needs to be translocated at the surface of the cells[64]. E-Selectin is not stored in the cells and must be transcribed upon receiving an inflammatory stimulus. The expression of E-selectin on the surface membrane can be found 3-6 hours after the initial stimulus[39].

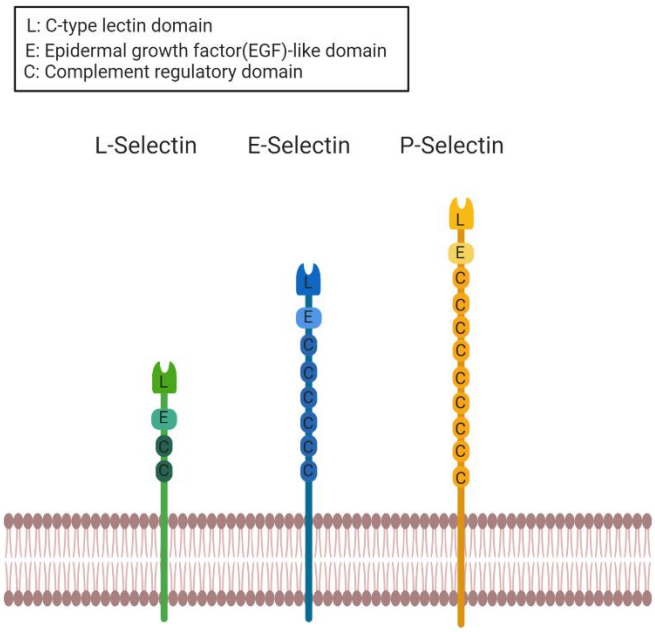

Figure 3. Structure of the selectins. Created with biorender.com

3.2. Selectin ligands

Endothelial selectins bind glycoproteins: P-selectin glycoprotein ligand-1 (PSGL-1) and E-selectin ligand 1 (ESL-1), also known as Golgi glycoprotein 1 (GLG1)[65,66]. PSGL-1 is a homodimer linked by a disulfide bond and possesses multiple o-glycans[67]. These ligands bind through an essential glycosylation motif called sialyl Lewis^x (sLex) described further. PSGL-1 can bind both P and E-selectin while ESL-1 can only bind E-selectin. P-selectin also possesses a second binding pocket that binds to sulfated tyrosines of PSGL-1[68].

3.3. The sialyl Lewis^x moiety

sLex is a tetrasaccharide composed of a fucose (fuc), an N-acetyl glucosamine (GlcNAc), a galactose (Gal), and an N-acetylneuraminic acid (NeuAc) subunits (Figure 4)[69]. The NeuAc unit is recognised by the selectins and binds to Tyr48 of the selectins. The GlcNac unit forms hydrogen bonds with Tyr94 and Glu92 of the lectin/EGF-like domains of the selectins. With P-selectin, NeuAc also forms a hydrogen bond with Ser99[70].

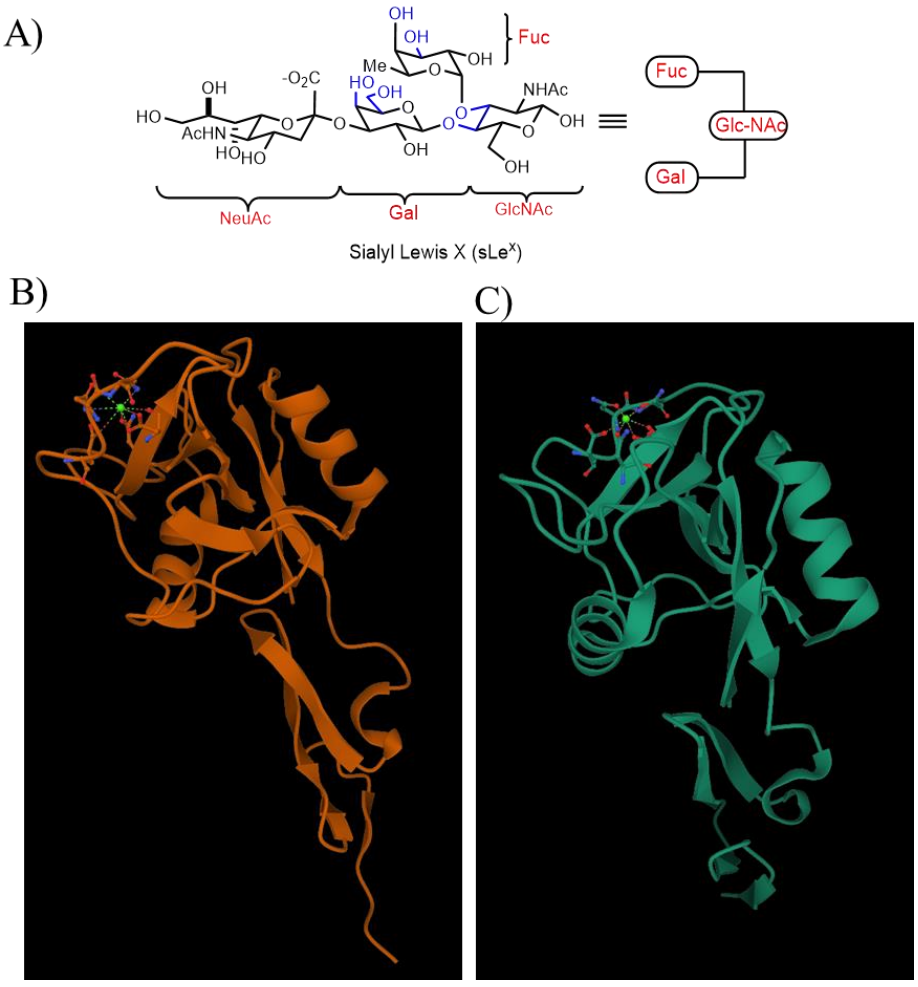

Figure 4. Lewis x moiety and binding to selectins. A) structure of sialyl Lewis x moiety. B) sialyl Lewis x docking on P-Selectin lectin and EGF domains. C) sialyl Lewis x docking on E-selectin

lectin and EGF domains. Protein structures and sLex docking were ontained using RCSB PBD (rcsbd.org) using Mol viewer using PDB ID: 1G1R and 1G1T respectively [70–72].

4. Selectins role in disease

The role of the selectins has been evaluated in various diseases[73–75]. Selectins have been found to play important roles in several inflammatory diseases such as in the vaso-occlusive crisis in sickle cell anemia, they have also been found to play a role in cancer metastasis[76,77]. Their role in these pathologies makes them an interesting candidate for the development of new inhibitors to reduce cellular recruitment.

4.1. Vaso-occlusive crisis in sickle cell anemia

Sickle cell anemia is a genetic disease that is characterized by an abnormal shape of red blood cells. It is due to a single nucleotide mutation in the beta-globulin (HBB), a sub-unit of hemoglobin, changing the arginine in the sixth codon to a threonine[78]. These red blood cells adopt a more elongated and rigid form instead of their healthy round bi-concave shape[79]. Patients with sickle cell anemia can experience a vaso-occlusive crisis. One of the key factors in this is the adhesion of multiple red blood cells on the microvascular walls. Patients with sickle cell anemia have a higher level of P-selectin expression in their endothelium[80]. The sickle red blood cells adhere to the selectin expressed on the endothelium[81]. Once the leukocytes bind to the endothelial cells through the selectins (both E and P), they express the macrophage-1 antigen (MAC-1) on their surface increasing their adhesion affinity to the vascular wall[75]. The accumulation of red blood cells, as well as platelets, creates a blockage in the vessel, thus causing a vaso-occlusive crisis (Figure 5). The blockage creates a hypoxic environment causing tissue damage and severe

pain. Patients experiencing these crises can require hospitalization. As discussed further, E-selectin antagonists have been synthesized in order to treat these crises but were unsuccessful. This can be explained by the important role that P-selectin plays in the development of these crises. There is currently no P-selectin antagonist available on the market.

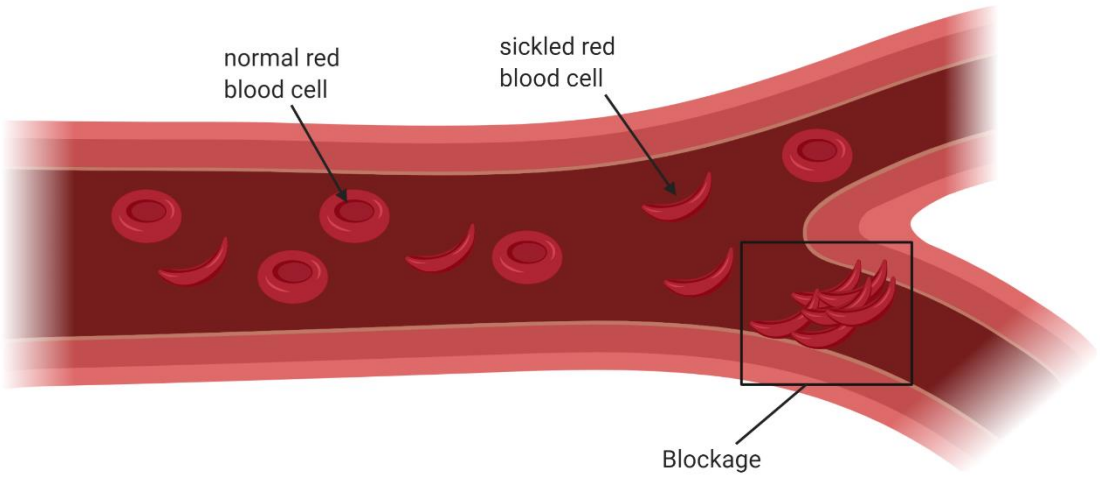

Figure 5. Schematic representation of vaso-occlusive crisis.

4.2. Cancer metastasis

Cancer refers to the presence of malignant tumors in the body. There are three types of cancers: carcinomas, lymphomas, and sarcomas, they are identified based on their tissue of origin[2]. Malignant tumors proliferate uncontrollably and will invade any surrounding tissue. These tumors can also produce metastasis. Metastasis occurs when a small group of cells detaches from the original tumor and invade the circulatory or lymphatic systems to reach other tissues[82]. In order to exit from the circulatory system, this group of cells will express various epitopes and ligands

involved in cellular recruitment such as, PSGL-1 and ESL-1. In most cancers, glycosyltransferase expression is up-regulated. Some of the common epitopes found on cancer cells are sLex and sialyl Lewis A (sLea)[83,84]. Using the sLex epitopes on their surface the tumor cells can use the adhesion molecules expressed during the inflammatory process in the order to invade other tissues. The interaction between cancer cells and P-selectin helps to promote their cellular adhesion. E-selectin helps to ensure efficient tumor extravasation of the metastases by ensuring an enhanced adhesion to the activated endothelium.[76]. The interaction with E-selectin leads to a loosening of the VE-cadherin junctions as well as an opening of the endothelial junctions[85]. The interaction with E-selectin increases the dephosphorylation of the Tyr371 of VE-cadherin. This dephosphorylation allows the induction of vascular permeability[86]. The amount of selectin ligand expressed on the surface of tumors has been well correlated with the presence of metastases in patients[76]. The selectins could represent a new target for therapies to reduce the instances of metastases in cancer.

5. Current anti-selectin treatments

As selectins play a role in several important diseases and play an important role in vascular inflammation making them a strong candidate for new anti-inflammatory treatments. Currently, there are no clinically available treatments targeting selectins. Two approaches are being developed: anti selectin antibodies or small molecule inhibitors.

5.1. Anti-selectin antibodies

One of the approaches to blocking selectin activity is to use an inhibitory antibody. Recently, several monoclonal antibodies are being developed as a treatment given their high specificity and low secondary effects[87]. Currently antibodies targeting the selectins are being developed[88]. These antibodies are designed to bind to an essential element of the selectin binding[88]. Blocking of the binding site then prevents other molecules to bind to the same target. Selexys is a p-selectin blocking antibody targeted against sickle cell anemia[88]. While antibodies can be very useful in several cancer treatments, they cannot concomitantly block both E and P-selectin interactions.

5.2. Small molecules antagonists

An approach in medicinal chemistry is the development of small molecules mimicking natural ligands. Glycomimetics consist of synthesising a molecule whose structure resembles the natural carbohydrate allowing the mimic to bind to the same targer[89]. The mimic compound, however, possesses a better pharmacological property than the natural carbohydrate[90]. Using this approach, it is possible to design molecules mimicking the structure of sLex. As previously described sLex attached to E and P-selectin ligands is an essential moiety in the selectin binding. Conceptualizing and preparing soluble sLex mimicking agents would then compete with the mentioned ligands by binding to the selectins. This would inhibit the affinity of immune cells to the vascular wall. The advantage of the small molecules over the antibodies is their ability to target both selectins making a pan-selectin antagonist. An additional benefit is the possibility to control the extent and duration of treatment. Various selectin antagonists have been synthesised, Bimosiamose (TBC-1269), OC-

226, and Rivipansel (GMI-1070) and are designed to help reduce inflammation and pain in various diseases[91,92].

5.2.1. Bimosiamose

Bimosiamose (Figure 6) was shown *in vitro* to inhibit all three selectins, P, E, and L[93]. In cellular rolling assays, TBC-1269 was able to reduce adhesion of murine myeloblastic cells to the murine P-selectin Fc[94]. In an induced peritonitis model (using thioglycolate) TBC-1269 was also found to reduce the number of infiltrated neutrophils[94]. However, using intravital microscopy it was unable to reduce leukocyte rolling in the cremaster venules of mice suggesting that its anti-inflammatory effects are mediated through a different mechanism[94]. This compound underwent phase II clinical trials for childhood asthma and psoriasis but failed to show any benefits[95]. Its failure may have been caused by the delivery system, through an aerosol, in combination with its low pharmacokinetics and stability in the bloodstream (half-life elimination of 4.1h)[96]. The low stability in the bloodstream indicates that this type of compound may not be suitable for the treatment of chronic inflammation through a daily regiment.

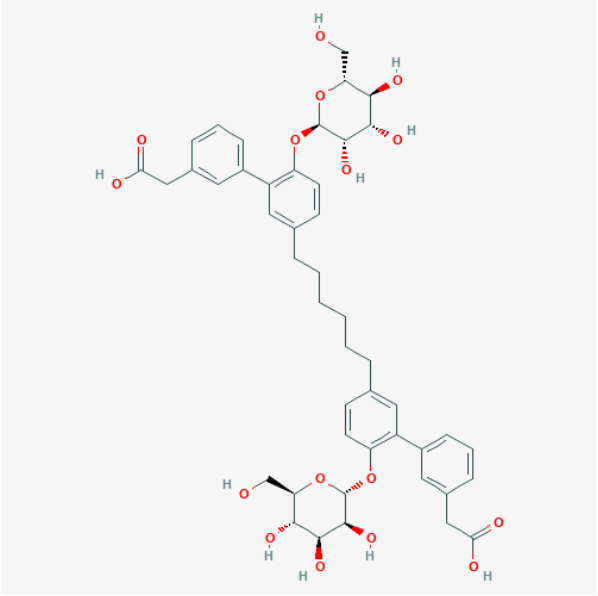

Figure 6. Structure of Bimosiamose (TBC-1269)

Rivipansel

Rivipansel (Figure 7) is another small molecule that binds very effectively to E-selectin (EC50 4μM) but does not bind very effectively to P-selectin (EC50 420μM)[91]. In intravital microscopy experiments, leukocyte velocity was increased in sickle cell anemia mice[92]. In mice treated with TNFα, GMI-1070 was found to inhibit the recruitment of leukocytes. It also reversed the vaso-occlusive crises, improving the blood flow of sickle cell anemia mice[91]. Phase III clinical trials have recently been completed on patients 6 years and older that require hospitalisation due to their vaso-occlusive crises. Rivipansel failed its primary outcome, which was the ability to reduce the time required to be able to discharge a patient. It also failed its auxiliary goals, reduce the consumption of opioids, and prevent re-hospitalisation within 3 days of patients' discharge[97]. This could be caused by its inability to block P-selectin that plays a major role in the adhesion of the red blood cells and platelets to the vascular walls.

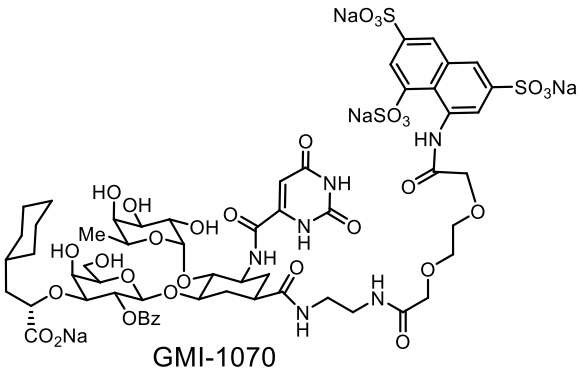

Figure 7. Structure of Rivipansel (GMI-1070).

5.3. Other compounds

Rivipansel appears to show some potential but it only binds E-selectin efficiently. Currently, there is no pan selectin antagonist that can effectively bind both vascular selectins. Our collaborators at the *Institut de Recherches Cliniques de Montréal* (IRCM) in Dr Guindon's laboratory have found a novel approach to design and synthesise new selectin antagonists mimicking sLex. In their compounds, the GlucNAC unit is replaced by an acyclic tether that possesses a conformational bias that mimics the bio-active one of sLex during binding with the selectins. Because of stereoelectronic effects, the fucose and galactose units attached to the tartrate are gauche to each other and stacked on top of each other as needed. The first generation of these molecules was found to bind both E and P selectin efficiently in surface plasmon resonance as well as in static and dynamic binding assays. In cremaster venules the leukocyte rolling was decreased[98].

Project Aims

The aim of my project was to evaluate the biochemical, cellular and *in vivo* abilities of a second generation of new selectin antagonists to bind E/P-Selectin and interfere with selectin-dependent immune cell recruitment to the endothelial wall. I also aimed to further characterize the role of GATA5 in vascular inflammation including selectin-dependent endothelial cell activation

Materiel and Methods

Animal work

All animal work and protocols were approved by the University of Ottawa animal care committee. Gata5-/- mice were previously described[54]. WT mice were obtained from Charles River Laboratories (C57BL/6, 027).

Cell culture

HDMEC were obtained from PromoCell® (C-12260) and cultured in MV2 media (PromoCell®, C-39226) in Primaria™ treated culture dishes (Corning, 087724F).

HL-60 obtained from ATCC® (CCL-240™) and cultured in IMDM (ATCC®, 30-2005™) with 20% FBS (Gibco™, 10082147) in tissue culture flasks (Falcon™, 13-680-59).

Cell-Selectin adhesion assay

Cell-selectin assays were carried out in 96 well plates. Wells were coated with 2ug/mL of homemade P-Selectin Fc or E-Selectin Fc in 3%BSA-TrisCa (50mM tris-HCl pH7.4, 150mM NaCl, 50mM $CaCl_2$). P-Selectin plates were coated overnight at 4°C while E-Selectin plates were coated 2h at 37°C. Plates were then blocked with a 1:1 solution of 3%BSA-TrisCa and StabiliCoat® (Sigma, S0950) for 1h at room temp with agitation. Simultaneously HL-60 cells were tagged with LeukoTracker™ (Cell Biolabs, CBA-210) and incubated 1h at 37°C in serum-free IMDM (ATCC, 30-2005). 10 000 HL-60 were then added to each well of the plate and left to incubate for 1h at 37°C. Our compounds or 50mM EDTA were then added at indicated concentrations and incubated for 30min at 37°C. Unbound cells were washed away and the plate was imaged using the Zeiss AxioObserver Z1 microscope (Carl Zeiss). Cells bound were counted

to determine binding and corrected over wells treated with EDTA using Fiji[99]. Inhibition was determined as 100%-binding observed.

Cell-Cell adhesion assays

Cell-Cell adhesion assays were carried out using the CytoSelect™ Leukocyte-Endothelium Adhesion Assay (Cell Biolabs, CBA-210) using the instruction provided. Briefly, HDMEC were seeded into a 96-well Primaria™ (Corning, 08-772-4K) plate and grown until the formation of a monolayer. Cells were then treated with 100ng/mL TNFα for 3h at 37°C. During the last hour of the TNF treatment, HL-60 cells were tagged with LeukoTracker™ at 37°C in serum-free medium. 10 000 HL-60 were added to each well of the plate and incubated for 1h at 37°C. Wells were then treated with our compounds, dissolved in 2% DMSO, at indicated concentrations to dislodge bound cells for 1h at 37°C. Unbound cells were washed away and remaining cells were lysed, and fluorescence levels were measured using SynergyH1 plate reader (BioTek) to determine binding. Inhibition was obtained using 100%-binding observed.

Surface plasmon resonance (SPR) binding assays

Molecular binding affinity analyses were performed using the Biacore X100 SPR system (GE Healthcare Life Sciences) equipped with CM5 sensor chips. Homemade P-Selectin Fc or E-Selectin Fc were immobilised using a standard amine coupling kit (GE Healthcare) according to the manufacturer protocol. Briefly, the surfaces of all flow cells were activated with NHS/EDC (1:1) for 7min. The ligands, P- or E-SelFc (30µg/mL and 25µg/mL, in 0.1M sodium acetate buffer at pH 4.3) were injected at a flow rate of 5µL/min for 7min on a single flow cell to achieve immobilised densities of 2200 RU and 1800 RU. Finally, all sensor chip surfaces were deactivated

with the injection of 1M Ethanolamine-HCl at pH 8.5. Blank reference flow cells without immobilised selectins were prepared. Before injecting the antagonists, the flow cells were equilibrated for 16 h in running buffer (10 mM HEPES at pH 7.4, containing 150 mM NaCl, 3 mM $CaCl_2$, and 0.005% (v/v) Surfactant P-20). For the ranking of binding affinity, SPR signals were recorded at a single concentration (1mM) with 120s association and dissociation time at 30µL/min over the reference cell. The average of the signal recorded at 95 s to 115 s after injection (plateau) was calculated and divided by the molecular weight of the analyte. A 60 s regeneration injection with 3.0M $MgCl_2$ was performed between each injection of analyte to prevent the presence of residual traces of compound in the system. Triplicate injections of each analyte were tested on the same sensor chip surfaces to determine standard error. In addition, two blank injections containing running buffer were included for each replicate. The data were processed with Scrubber 2.0c (BioLogic Software). Double referencing (subtraction of reference surface and blank injection) was applied to correct bulk effects and other systematic artifacts. The analysis was performed by Ryan Simard in the Guindon laboratory (IRCM).

***In vivo* cell migration assay**

Cell migration assay was carried out as described by Ray and Dittel[100]. Briefly, mice were injected with 1mL 3% thioglycolate (Sigma-Aldrich, 70157) in the peritoneal cavity. After 10min the mice were injected with saline, sLex (Carbosynth, OS04058), or compounds at indicated concentrations through IV. Mice were left for 2h before being sacrificed. The skin of the peritoneal cavity was removed and the cavity was washed with 5mL of 2% heat-inactivated FBS 1X PBS (Gibco, 70013-032), PBS was collected and red blood cells were lysed with Red Blood Cell Lysing Buffer Hybri-Max™ (Sigma-Aldrich, R7767). 1 million cells were used for identification by flow cytometry.

Neutrophils were identified using a live/dead marker (), and several surface proteins known to be present or absent on neutrophils allowing their identification: PSGL1+, CD11b+, CD11c-, Ly-6C+, Ly-6G+.

HDMEC GATA5 KD cell generation

Knockdown cells were generated as previously reported by Messoudi and al[55].

HDMEC GATA5 overexpression cell generation

Control and GATA5 viral shRNA plasmids were obtained from Addgene (20672, 105508). Viral particles were generated by co-transfection of phoenix cells with the packaging vectors psPAX2 and pMD2G using effectene (Qiagen, 301425). Twenty-four hours after transfection media was replaced by endothelial growth medium 2 (PromoCell). Forty-eight hours after media was collected and filtered and used for infection of HDMECs. Infected cells were selected using puromycin 2.5ug/ml until all cells in non-transfected plate were killed. Cells were maintained in puromycin 0.25ug/mL.

RT-QPCR

Transcript levels were determined by real time PCR using procedures described by Debrus et al[101].

Table 1. List of human primers

E-selectin	forward	CAGAAAGTCCAGCTACCAAGG
	reverse	AAGTTCGCCTGTCCTGAAG

P-selectin	forward	ACGCTGGATTCACACTCATAG
	reverse	AGAGGTTGGAGCAGTTCATC
GATA5	forward	AAGCATCCAGACACGGAAGC
	reverse	CTTTCGAAGTGGCTGCTGAG
MYH10	forward	AGCCCAGACCAAAGAACAG
	reverse	ATGAAAGATGCTCCCTGACG
OCLN	forward	GCAAAGTGAATGACAAGCGG
	reverse	CACAGGCGAAGTTAATGGAAG
PRKACB	forward	CCTTTCCTTGTTCGACTGGAG
	reverse	TGAGCTGCATAGAACCGTG
TJP1	forward	CGAAGGAGTTGAGCAGGAAA
	reverse	ACAGGCTTCAGGAACTTGAG
TNFRSF1B	forward	GTCCACACGATCCCAACAC
	reverse	TGTCACACCCACAATCAGTC

CLDN1	forward	TTGACTCCTTGCTGAATCTGAG
	reverse	TTCTGCACCTCATCGTCTTC
MYL9	forward	TGATTGACCAGAACCGTGATG
	reverse	TGGTGAGGAACATGGTGAAG
MYLK	forward	TTAGAAGTTGTGGAGGGAAGTG
	reverse	GTAGTCTATCTGGAAGTGGCG
F2RL2	forward	TCCTCATCTCCCTTCCAACTC
	reverse	TCGCCTTAACATACCACAACC
PRCKI	forward	ACTACGGCATGTGTAAGGAAG
	reverse	TCAAACATGAGCACTCCAAGAG
ABCA1	forward	AACGAGACTAACCAGGCAATC
	reverse	ACACAATACCAGCCCAGAAC
BIRC5	forward	TAATACCAGCACTTTGGGAGG
	reverse	GGCTCTTTCTCTGTCCAGTTTC

CLU	forward	ATTCAAAATGCTGTCAACGGG
	reverse	CTTTGTCTCTGATTCCCTGGTC
SPHK1	forward	AGGCTGAAATCTCCTTCACG
	reverse	CTCCATGAGCCCGTTCAC
PLAT	forward	ACTTCCCAGCAAATCCTTCG
	reverse	AGGACAAGAAACACGTCTGG
COL1A2	forward	GGTGATGTTCTGAGAGGCATAG
	reverse	GGTGATGTTCTGAGAGGCATAG
IL1A	forward	TGTATGTGACTGCCCAAGATG
	reverse	TTAGTGCCGTGAGTTTCCC
ITGB8	forward	CGTCTCATCTCGCTCTTGATAG
	reverse	TTCTCTGAAAGTTGGCCTAGTG
ICAM1	forward	GGTAGCAGCCGCAGTCATAA
	reverse	GATAGGTTCAGGGAGGCGTG

Table 2. List of mouse primers

E-selectin	forward	GCTGGAGAACTTGCGTTTAAG
	reverse	AGATAAGGCTTCACACTGGAC
P-selectin	forward	TTTGGCTTCTGGGATCTGG
	reverse	GGCTGGCACTCAAATTTACAG
MYH10	forward	AGAAACACTGACCAAGCCTC
	reverse	ATCACATTCATCCCGAGCAG
OCLN	forward	AAACTGGTTGCAGATCATATAT
	reverse	GTGTTTATTGCCACGATCGTGT
PRKACB	forward	AGGGTTACAATAAGGCGGTG
	reverse	TGAAGTGTGATGGGAACCG
TJP1	forward	AGCGAATGTCTAAACCTGGG
	reverse	TCCAACTTGAGCATACACAGG
TNFRSF1B	forward	ACTCCAAGCATCCTTACATCG
	reverse	TTCACCAGTCCTAACATCAGC

CLDN1	forward	AGGTCTGGCGACATTAGTGG
	reverse	CGTGGTGTTGGGTAAGAGGT
MYL9	forward	ACAGCGCCGAGGACTTTTC
	reverse	AGACATTGGACGTAGCCCTCT
MYLK	forward	TTGTGGCTCCTGAAGTGATC
	reverse	TGAAGTGACGTTGGCTAAGG
F2RL2	forward	GTTTCTGCCAGTCACTGTTTG
	reverse	TGTCCAGCCCTCTATGTCAG
PRCKI	forward	GAAGCATGTGTTTGAGCAGG
	reverse	AGGAAGTTTTCTCTGTCGCTG
ABCA1	forward	TGACATGGTACATCGAAGCC
	reverse	GATTTCTGACACTCCCTTCTGG
BIRC5	forward	AAGGAATTGGAAGGCTGGG
	reverse	TTCTTGACAGTGAGGAAGGC

CLU	forward	AAAGTGCCAGGAGATCTTGTC
	reverse	CATGTTCGACTGGAAGGACTG
SPHK1	forward	TGAATGGGCTAATGGAACGG
	reverse	GTCTTCATTAGTCACCTGCTCG
PLAT	forward	GAAACCCAGACCGAGACTTG
	reverse	TCACACCTTTCCCAACATAGC
COL1A2	forward	AAGGATACAGTGGATTGCAGG
	reverse	TCTACCATCTTTGCCAACGG
IL1A	forward	TGCAGTCCATAACCCATGATC
	reverse	ACAAACTTCTGCCTGACGAG
ICAM1	forward	GTGTCGAGCTTTGGGATGGT
	reverse	GGAGCCAATTTCTCATGCCG

Western Blot

Proteins from HDMEC were obtained using whole-cell extracts as previously described[101].

Proteins from lung endothelial cells were obtained using QIAzol™ using protocol described by Kopec *et al*[102].

ICAM1 human antibody was obtained from Abcam (ab2213), ICAM1 mouse antibody was obtained from Abcam (ab171123), Survivin antibody was obtained from Abcam (ab469), OCLN antibody was obtained from LSBio (LS-B2320), TJP1 antibody was obtained from Novusbio (NBP1-85047), CLDN1 antibody was obtained from Abcam (ab15098).

RNA extraction

RNA was extracted using QIAzol™ reagent (Quiagen, 79306) using instructions provided by the manufacturer.

cDNA generation

cDNA was obtained using the QuantiTect® Reverse Transcription kit (Quiagen, 205313) using manufacturer instructions.

Homemade Selectin generation

The protein generation and purification were performed by Janie Beauregard. Briefly, full-length selectins (P and E) were cloned in the pFUSE-hlgG1-Fc1 plasmid (using AgeI, EcoRV and AgeI, BglII respectively). Plasmids were then transfected in AD293 cells using effectene using instructions provided by manufacturer. Transfected cells were selected in 400µg/mL ZEOCIN. The proteins were secreted in the media. Media was collected and the proteins were concentrated

using Amicon Ultra centrifugal columns (Milipore, UFC903024). Selectins were purified on HiTrap® Protein G columns (GE Healthcare, 17-0404-01) using the manufacturer's instructions. The elution was buffer exchanged to 1X PBS using Amicon columns.

Flow Cytometry

Flow Cytometry experiments were performed on an LSR Fortessa™ (BD Biosciences). PSGL-1 antibody was obtained from BD Pharmigen (562806). CD11b antibody was obtained from BD Pharmigen (563402). CD11c antibody was obtained from BD Pharmigen (563735). Ly-6C antibody was obtained from BD Pharmigen (560592). Ly-6G antibody was obtained from. Viability dye was obtained from BD Pharmigen (565388). CD62p antibody was obtained from BD Parmigen (555523). CD62e antibody was obtained from BD Pharmigen (563360). Results were analysed using FlowJo V10.

Lung endothelial cell isolation

Endothelial cells were isolated using a protocol from Pang[103]. Briefly, mice were anesthetised and sacrificed by cervical dislocation. Thoracic cavity was then opened, and lungs were extracted and put in ice-cold DMEM. Lungs were then minced and put into digestion solution (1mg/mL collagenase I, 10mg/mL BSA, 1U/mL dispase in DMEM) for 15min with agitation at 37˚C. The solution was mixed with up/downs every 15min 3X. Cells were then re-minced into less than 1mm size pieces and kept in digestion solution at 37˚C. The solution was exchanged every 5min. Cells were then plated into tissue culture treated plated for 1h at 37˚C. Unbound cells were collected and incubated with anti-CD31 coated beads (Invitrogen, 11155D). Cells bound to beads were plated on Primaria™ coated tissue culture plates (Corning, 08-772-4J) in culture growth medium (20%

FBS, 10μg/mL ECGS (Sigma-Aldrich, E2759), 100UmL Antibiotic (Invitrogen, 15140-122), 20U/mL heparin (Sandoz, 10750) in F12 medium).

Statistical Analysis

Data are reported as mean ± SEM. Statistics were obtained using unpaired student t-test for two-group comparison. For multiple groups, one-way ANOVA test was used. P-value of <0.05 was considered significant

Results

6. Evaluation of potential new selectin antagonists

The first aim of this project was to evaluate the efficacy of potential novel selectin antagonists synthesised by our collaborators in the "*Laboratoire de chimie bio-organique*" of Dr Guindon laboratory in the IRCM. We evaluated the compounds in *in vitro* assays as well as *in vivo* assays using cell culture and a mouse model. The new compounds, based on the lead compound of the first generation (LCB 111), can be divided into three classes (Figure 8). The first class contains a modified sialyl Lewis x core (tartrate replacement) to which an anionic side chain was added. The side chains are aimed at the second binding pocket, containing the sulfated tyrosines, of the PSGL-1 which should also improve P-selectin binding. The second class consists of modifying the sLex core in order to lock the carboxylic acid attached to the galactose in its bioactive pre-organising the conformation of Sialyl Lewis X binding to P-selectin. Pre-organising the configuration of the carboxylic acid by making bicyclic molecules should increase the binding of these antagonists. Finally, the third class consists of the combination of the more effective core of the second class with the best anionic side chain of the first generation.

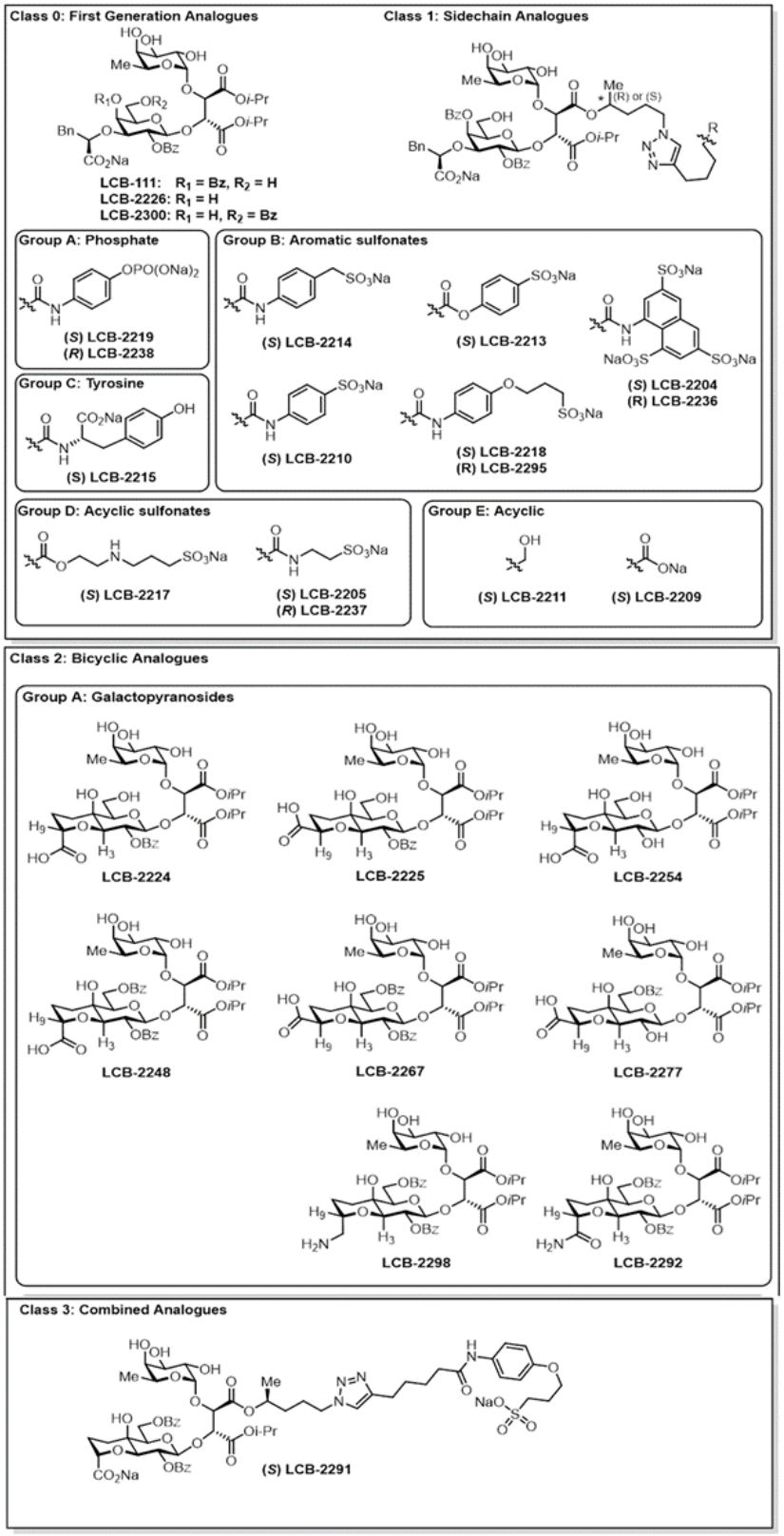

Figure 8. Structures of novel selectin antagonists.

6.1. *In vitro* binding

The first assay we used to evaluate our molecules was an *in vitro* binding assay, using surface plasmon resonance (SPR) technology in collaboration with Ryan Simard form Dr Guindon laboratory at the IRCM. This assay allowed us to measure the direct binding affinities to E and P-selectin individually. To perform this, a BiaCore X-100 instrument along with CM5 chips were used. The CM5 were coated with either E or P-selectin and the compounds were passed at 1mM at 30µL/min over the coated chips (Figure 9). The interaction between the selectins and the compounds will alter the angle of the reflected light captured on the detector. Binding affinities of our compounds were determined once the binding reached its plateau (between 95-115 seconds) after their injection in the flow cell.

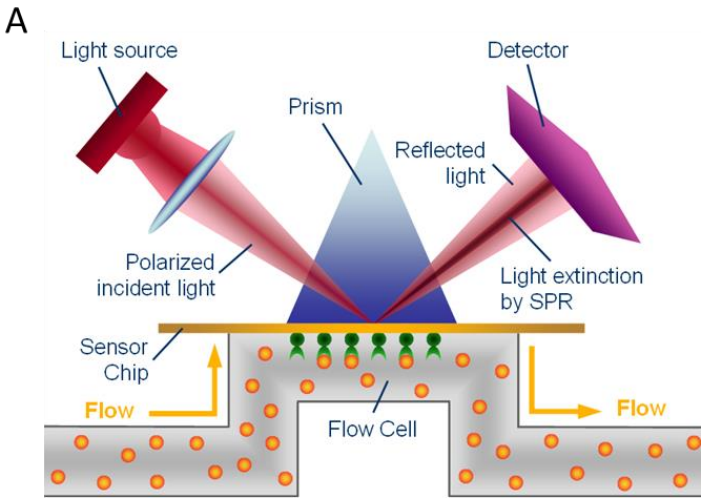

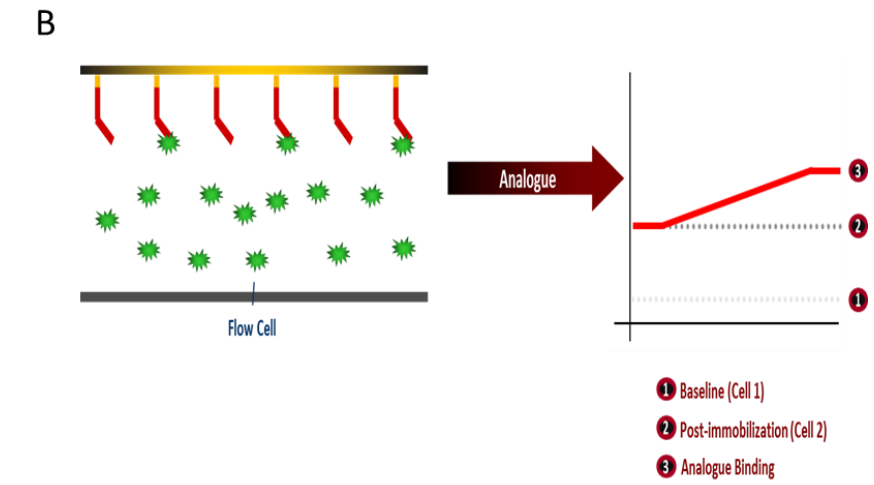

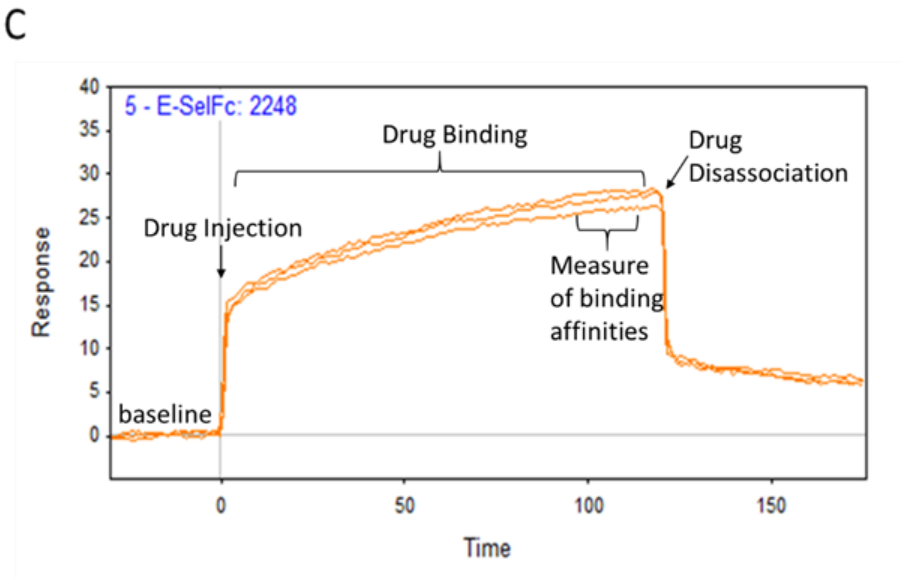

Figure 9. Surface plasmon resonance (SPR) experimental design. **A.** Schematic of SPR experiment. **B**. Schematic representation of signal observation. **C**. Results obtained with LCB2248 on E-Selectin of three analytical repeats

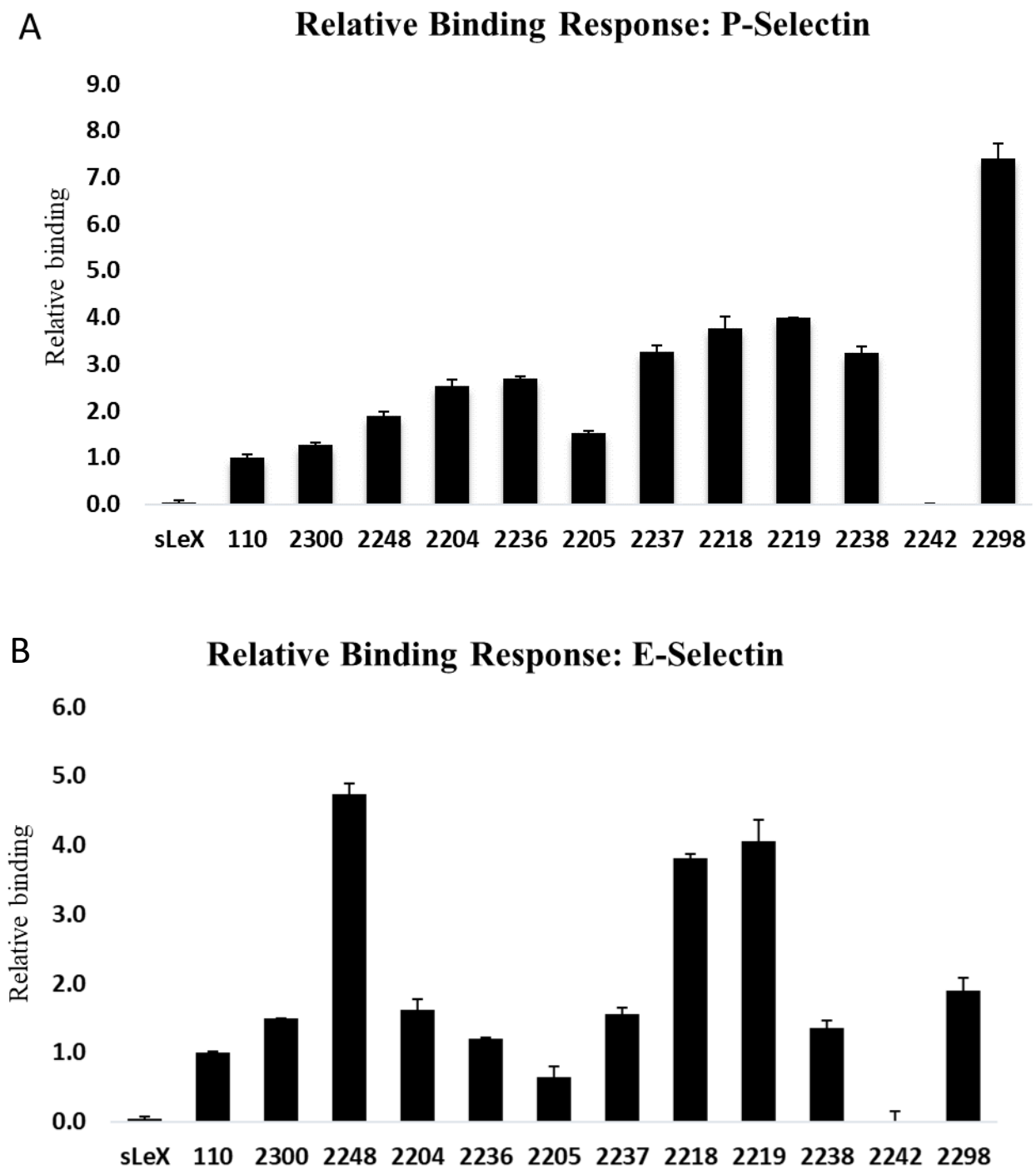

Figure 10. Binding assays of 18 new compounds using SPR. The results shown represent the data obtained at a concentration of 1 mM and is expressed relative to the lead LCB-110 molecule arbitrarily set to 1 (SPR signal divided by the molecular weight and normalized to 110). **A)** P-selectin binding affinity. **B)** E-selectin binding affinity. Results are the mean (±SEM) of three analytical repeats.

The results, shown in Figure 10, indicate that most of our compounds bind more effectively than the previous generation of molecules (LCB 110) to both E and P-selectin. Furthermore, we observe that the molecules containing an anionic side chain (LCB 2204, 2236, 2205, 2237, 2218, 2219, 2238) bind more effectively to P vs E-selectin. This may suggest that these molecules bind to the sulfate tyrosine pocket or to another positively charged region of the P-selectin protein. The molecules with the side chains are attached on a chiral carbon. Chiral carbons are designated when the molecule cannot be superimposed in its mirror image[104].The presence of a chiral carbon allows us to attach the chain in two different configurations (or enantiomers). These configurations are determined by their special arrangement of the substituent group around the carbon whether they rotate plane-polarised light in a right or left handed manner[104]. The configuration of the molecule could influence the binding affinity of the compounds with the same structures. Indeed, LCB 2219 shows a much higher affinity to E-selectin and a small increase to P-selectin compared to its R isomer, LCB 2238. LCB 2205 (S) and 2237 (R) also show differential activity towards E- and P-selectin except that in this case, the R isoform has a stronger affinity. There was no difference between the R and S configuration of LCB 2204 and LCB 2236. An increase in the binding to E-selectin was unexpected in the first class of molecules as this vascular adhesion protein does not possess the sulfated tyrosine pocket that the side chains are designed to bind with. As for the bicyclic molecules (LCB 2248, 2242, and 2298), LCB 2248 and 2298 show improved binding to both E and P-selectin while LCB 2242 does not appear to be able to bind to either selectin. This may be due to the different groups attached on the C9 position: LCB 2248 has a carboxyl, LCB 2298 has an amine while LCB 2242 has a tetrazole.

6.2. Cellular binding assays

The SPR assays allow us to determine the ability of the molecules to bind directly to the selectins. However, the cellular environments and dynamics can influence both selectin binding and its biological consequences. In order to analyse the potential *in vivo* effects of our molecules, we first tested them using cellular assays. The first assay measures the inhibitory capacity of our molecules to block the binding of leukocytes to the selectins directly (cell-protein assays). The second assay aims at evaluating the inhibitory capacity of blocking the adhesion of leukocytes to endothelial cells (cell-cell assays).

6.2.1. Cell-protein binding assays

The first step to mimic *in vitro* the interaction between leukocytes and endothelial selectins cells was to coat 96-well culture plates with either E or P-selectin. Human leukocyte like cells (HL-60) were then added to bind to the selectins. HL-60 cells are commonly used in cellular binding assays and are known to express PSGL-1 and ESL-1 at their surface making them a good model for the evaluation of our molecules. The ability of our molecules, LCB 111, 2218, 2219, 2237, 2248, 2251, 2267, 2242, 2224, 2225, 2294, and 2291, to inhibit the binding was determined by their ability to dislodge the bound HL-60 (Figure 11). As the plates were coated with only one of the selectins, we were able to measure the specific inhibitory potential of our molecules against either E or P-selectin individually. The results for the different classes of molecules are shown in Figure 12 and the IC50s are displayed in table 1.

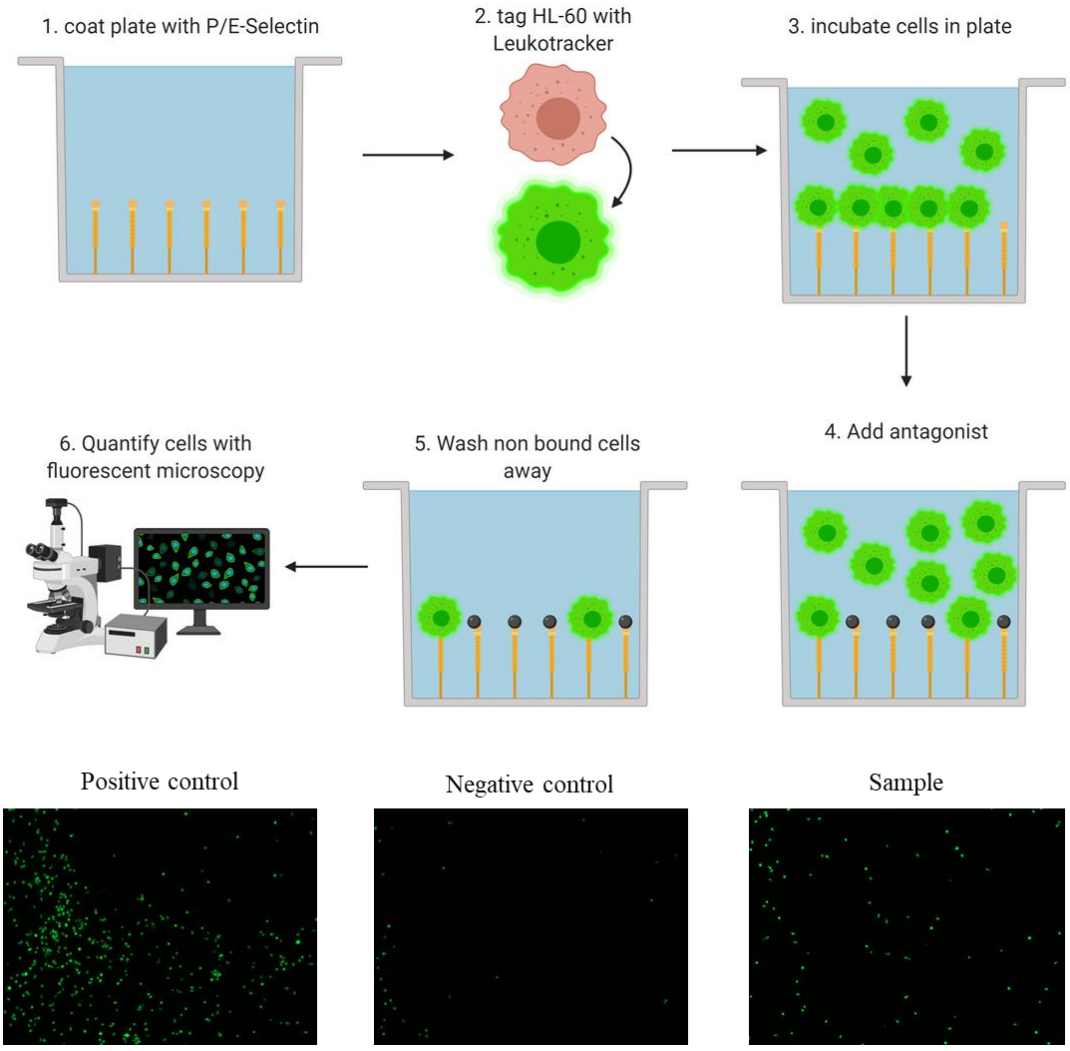

Figure 11. Schematic of the experimental procedure used for the cell-selectin assay

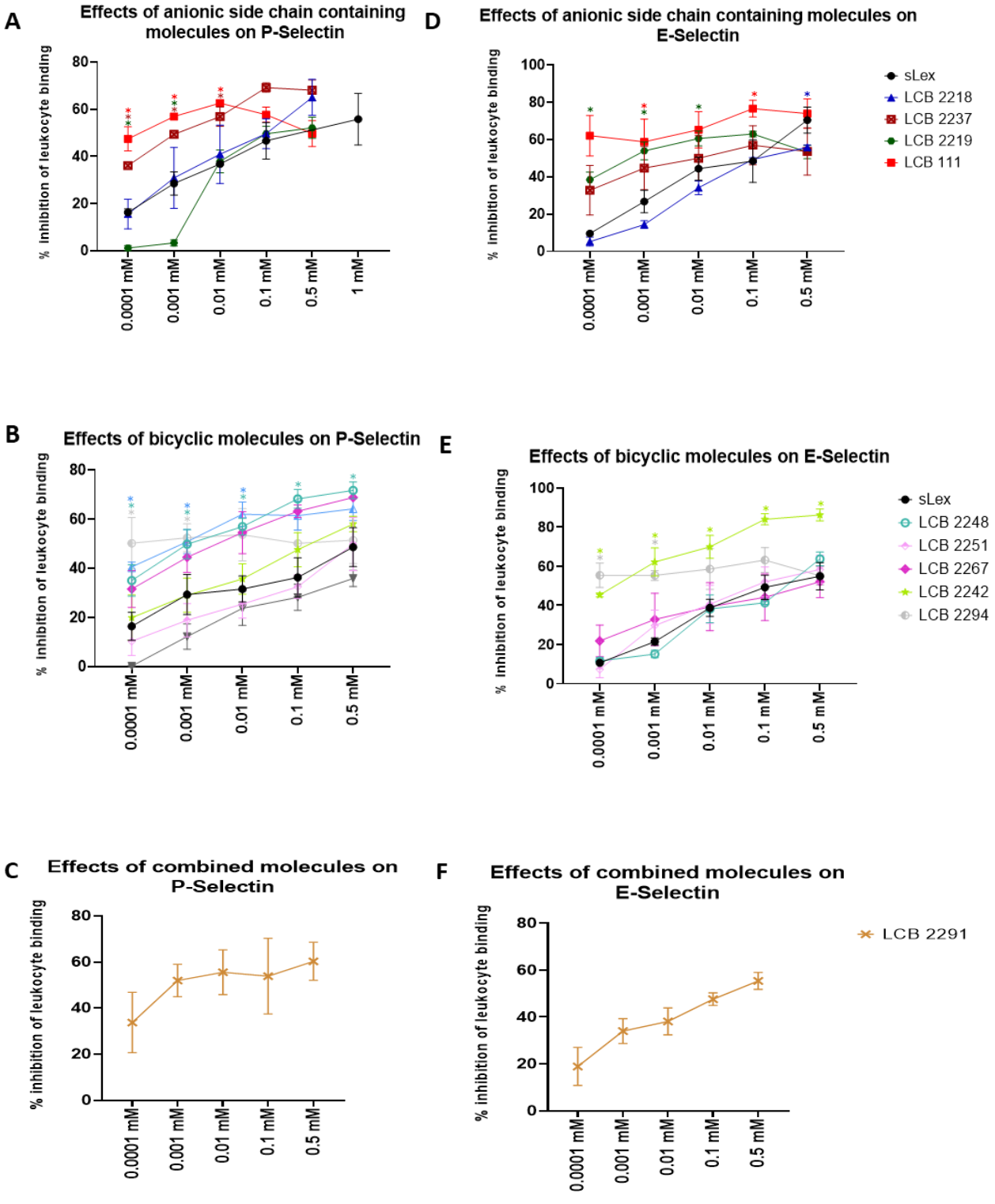

Figure 12. Selectin cell-based adhesion assays. 2ug/mL of P or E-Selectin was coated on 96 well plates. Fluorescently tagged HL-60 with LeukoTracker were then incubated for 1 hr with either E- or P- selectins. Antagonists were added for 30 min at the indicated concentrations to dislodge

bound cell. %inhibition was calculated as 100%-%binding observed by fluorescence. **A)** Cell- P-selectin treated with anionic side chain molecules. **B)** Cell- P-selectin treated with bicyclic core molecules. **C)** Cell- P-selectin treated with combined side chain and bicyclic core molecule. **D)** Cell- E-selectin treated with anionic side chain molecules. **E)** Cell- E-selectin treated with bicyclic core molecules. **F)** Cell E-selectin treated with combined side chain and bicyclic core molecule. Results are mean (±SEM) of three independent experiments normalised to respective external controls. Significance was determined in comparison with sialyl Lewis x (sLex). *p<0.05

Table 3. IC50 antagonists evaluated in cell-protein assay.

Antagonist	[IC50] P-Selectin	[IC50] E-selectin	[IC50]/[IC50 sLex] P-Selectin	[IC50]/[IC50 sLex] E-Selectin
sLex	1.2 µM ± 3.04	4.2µM ± 1.49	1	1
LCB 2218	2.0 µM ± 3.03	4.7 µM ± 0.61	1.67	1.11
LCB 2237	0.04 µM ±0.04	4.8 nM ± 2.91	0.03	0.001
LCB 2219	5.8 µM ± 1.43	0.1 nM ± 0.02	4.84	0.000001
LCB 2248	0.07 µM ± 0.08	6.0 µM ± 2.99	0.06	1.42
LCB 2251	4.8 µM ± 4.98	1.7 µM ± 1.28	4.00	0.41
LCB 2267	0.13 µM ± 0.09	0.2 µM ± 2.67	0.11	0.05
LCB 2242	1.0 µM ± 2.87	0.03 µM ± 0.03	0.90	0.008
LCB 2224	5.1 µM ± 5.07	-	1.25	-
LCB 2225	1.4 nM ± 0.004	-	0.001	-
LCB 2291	2.4 nM ± 0.18	0.5 µM ± 1.28	0.002	0.13

It is possible to observe that different molecules are more effective against E and P-selectin. In the first class, the anionic side chains, LCB 2237 is the more effective molecule to inhibit the cellular adhesion against P-selectin. This suggests that the acyclic sulfonate side chains are the most effective P-selectin inhibitors. In contrast, LCB 2219 binds more effectively to E-selectin indicating that the aromatic sulfonates are more effective at inhibiting the E-selectin interaction.

These results are consistent with those obtained in the SPR binding assays which revealed that the aromatic and acyclic sulfonates had the most affinity to the selectins.

The bicyclic cores also bind differently to E and P-selectin. LCB 2248 binds very effectively to P-selectin while LCB 2242 binds much better to E-selectin than the other compounds. The activity of LCB 2242 was unexpected as it did not seem able to bind the selectins in the *in vitro* assays. The bicycle molecules inhibit cellular binding to both E and P-selectin more effectively than the molecules of the anionic class of molecules. This suggests that locking the carboxylic group in the active configuration is more effective than the binding to the sulfated tyrosines.

In the third generation, LCB 2291, the combination of the LCB 2248 core and the LCB 2218 side chain does not show an increase in the maximal inhibition compared to LCB 2248. This unexpected result suggests, that the increased binding provided by the anionic side chains and that obtained with the bicyclic cores are not synergistic and do not further increase the inhibitory action of our molecules.

6.2.2. Cell-cell binding assays

After evaluating our molecules ability to dislodge the HL-60 from the selectins directly we used a cell-cell assay to mimic the interactions found in the blood vessel between leukocytes and endothelial cells. This assay allows us to evaluate the ability of our compounds to block the

recruitment of immune cells on the surface of blood vessels[105]. We used human dermal microvascular endothelial cells (HDMEC) for this assay. The HDMEC were coated to form a monolayer to represent the vessel surface and treated to selectively upregulate either E or P-selectin. Unlike E-selectin, P-selectin does not possess an NFκB element in its promoter; consequently, treatment with TNFα stimulates E-but not P-selectin[106]. To confirm the specificity of our treatments, HDMECs were treated with 100ng/mL of TNFα for 3h and the cells were stained for E and P-selectin expression and measured by flow cytometry. In addition, the total RNA was also extracted, and changes in mRNA of E and P-selectin induced by the TNFα was measured by QPCR. As shown in Figure 13, E-selectin mRNA was increased by 280 folds (lower panel) and surface protein expression was increased by 50 folds (top panel) while P-selectin levels were unchanged. Unfortunately, no treatment was found to specifically and reproducibly stimulate P-selectin possibly due to its rapid and transient profile. Therefore, we used TNFα stimulated endothelial cells to which we added HL-60 cells to evaluate our molecules ability to dislodge leukocytes from the E-selectin in endothelial cells.

A

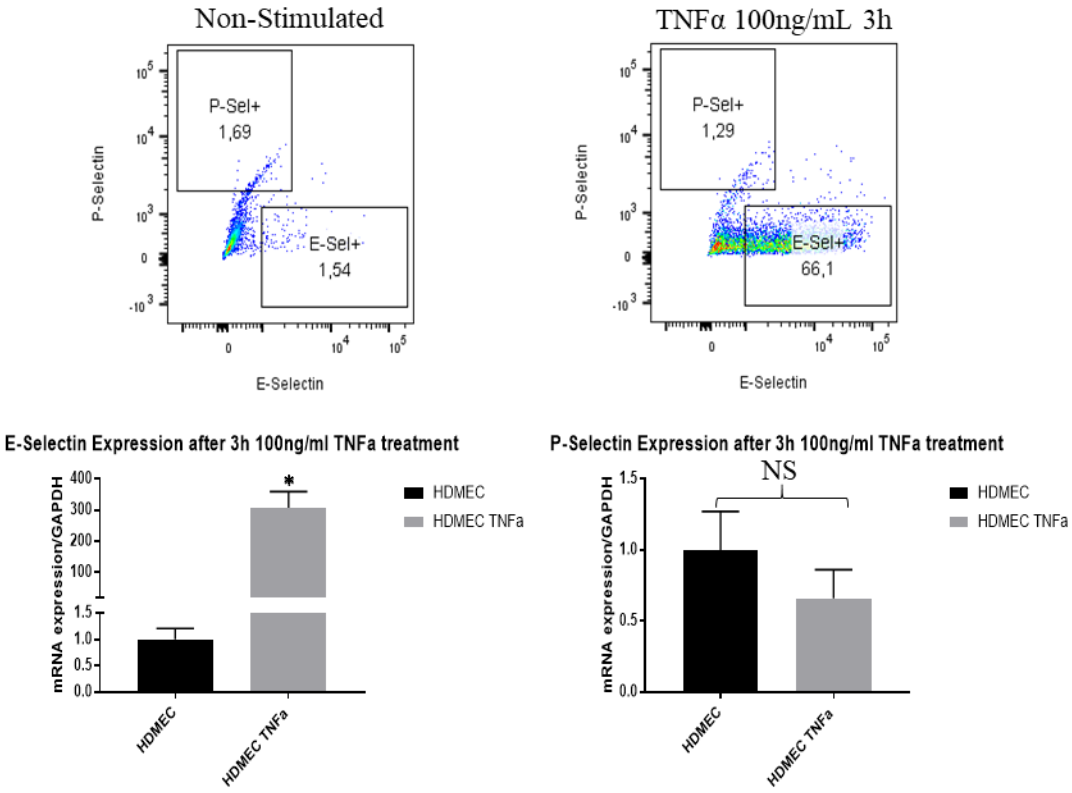
Non-Stimulated
TNFα 100ng/mL 3h
P-Sel+
1,69
E-Sel+
1,54
P-Sel+
1,29
E-Sel+
66,1
P-Selectin
E-Selectin
E-Selectin Expression after 3h 100ng/ml TNFa treatment
P-Selectin Expression after 3h 100ng/ml TNFa treatment
mRNA expression/GAPDH
HDMEC
HDMEC TNFa
NS
*

B

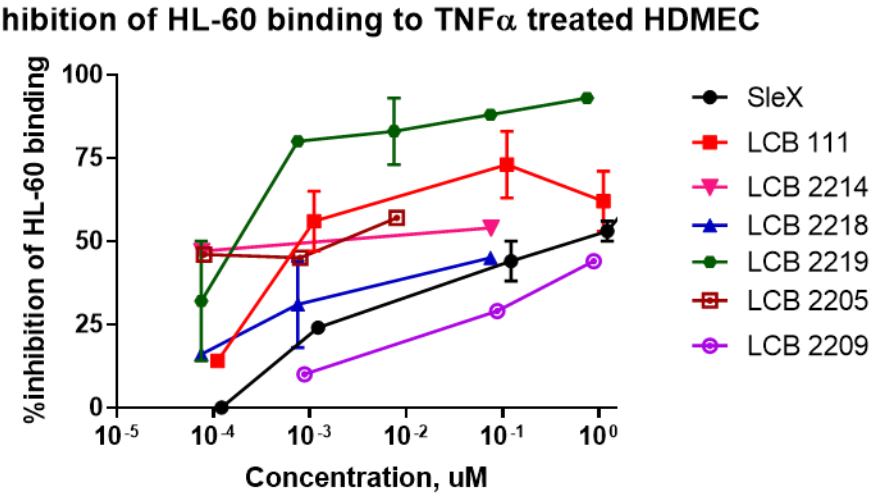
Inhibition of HL-60 binding to TNFα treated HDMEC
%inhibition of HL-60 binding
Concentration, uM
SleX
LCB 111
LCB 2214
LCB 2218
LCB 2219
LCB 2205
LCB 2209

Figure 13. Cell-cell adhesion assays. **A)** expression of E- and P-selectin on HDMEC cells after 3 hours of 100ng/mL TNFα treatment using flow cytometry (protein level, upper panel) and QPCR (relative mRNA levels, lower panels) **B)** cell-cell static binding assays of HDMEC treated with 100ng/mL TNFα (3h) and LeukoTracker® labelled HL-60s followed by 1h treatment with the various compounds at varying doses. Cells were lysed 5min and fluorescence was measured using Synergy H1 plate reader to determine binding. % Inhibition was determined as 100% - % residual binding. Results are the mean (±SEM) of three separate experiments normalised to their respective controls. *$p<0.05$

In the cell-cell adhesion assay, LCB 2219 was the most effective compound reaching a maximum inhibition of 88%. LCB 2218 does not show an ability to inhibit the binding of the HL-60 to the HDMEC. LCB 2205 shows a much stronger inhibition than sLex at the low doses which LCB 2209 was less effective than sLex. The inefficient binding of LCB 2209 is most likely due to the short length of the side chain attached that was not able to reach and bind with the sulfated tyrosines. As the SPR assays show LCB 2237 has a stronger affinity than LCB 2205, suggesting that LCB 2237 would have a very strong inhibitory potential. LCB 2237 and the bicyclic molecules remain to be tested.

6.3. Cellular migration assay

Finally, the last assay we used to evaluate our molecules was the peritoneal lavage mouse model. The peritoneal lavage allows us to measure the number of cells that migrate from the blood vessels to the peritoneal cavity after an inflammatory stimulus of thioglycolate is administered[107]. The peritoneal lavage mouse model is a well-established assay that is commonly used to evaluate cellular migration of various inflammatory cell populations[108,109]. The various inflammatory cell populations recruited can be then identified using flow cytometry, based on staining for a combination of surface proteins. We focused on two main populations: all the PSGL-1 positive

cells and the neutrophils ($CD11b^+$, $CD11c^-$, $Ly\text{-}6C^+$, and $LY\text{-}6G^+$) (Figure 14). We focused on PSGL-1 positive cells as our molecules are designed to inhibit the interaction of PSGL-1 molecule with the vascular selectins. We focused on the neutrophils as they are the first immune cell population to be recruited in any inflammatory response. In order to focus on migrating inflammatory cells, we collected them two hours post-stimulation. This short time ensured the cells did not have time to divide or differentiate. While most LCB compounds showed a strong inhibitory potential in the cellular assays, only a few showed activity in the mice model as shown in figure 15. In part that could be due to the rate of metabolic degradation when given intravenously or to the differential interaction with factors present in the *in vivo* model, including flow conditions.

With respect to the neutrophil population, only LCB 2248 treatment resulted in a significant reduction at all the tested dosages. While LCB 2248 and 2267 have the same carboxyl group on the C9 position but it is in a different orientation. LCB 2248 has the group in an axial position while LCB 2267 is in an equatorial position, demonstrating that under flow condition the group orientation could play an important role in the ability of our molecules to bind to the vascular selectins. Several other compounds (LCB 2218, 2242, and 2291) only lead to a reduction of neutrophils at one dosage at which they were evaluated; 2.5µmol/kg (2218, 2242) and 0.25µmol/kg (2291). Interestingly, the reduction is only found at the lower dosages evaluated. Surprisingly, LCB 2219 treatment led to an increase in the neutrophil population recruited, effectively acting as an agonist instead of an antagonist. In the PSGL-1 population, only one compound showed a significant reduction, LCB 2248, at all three of the tested dosages. Just like in the neutrophil population, LCB 2219 showed a significant increase in the PSGL-1 population.

LCB 2248 has shown strong affinity to both selectins in the *in vitro* assay as well as a strong inhibitory potential against P-selectin in the selectin adhesion assays. LCB 2248 is also the only compound that was able to reduce both the neutrophil and PSGL-1 cell populations in the peritoneal lavage in a dose-dependent manner, thus LCB 2248 stands out as the lead candidate for further evaluation.

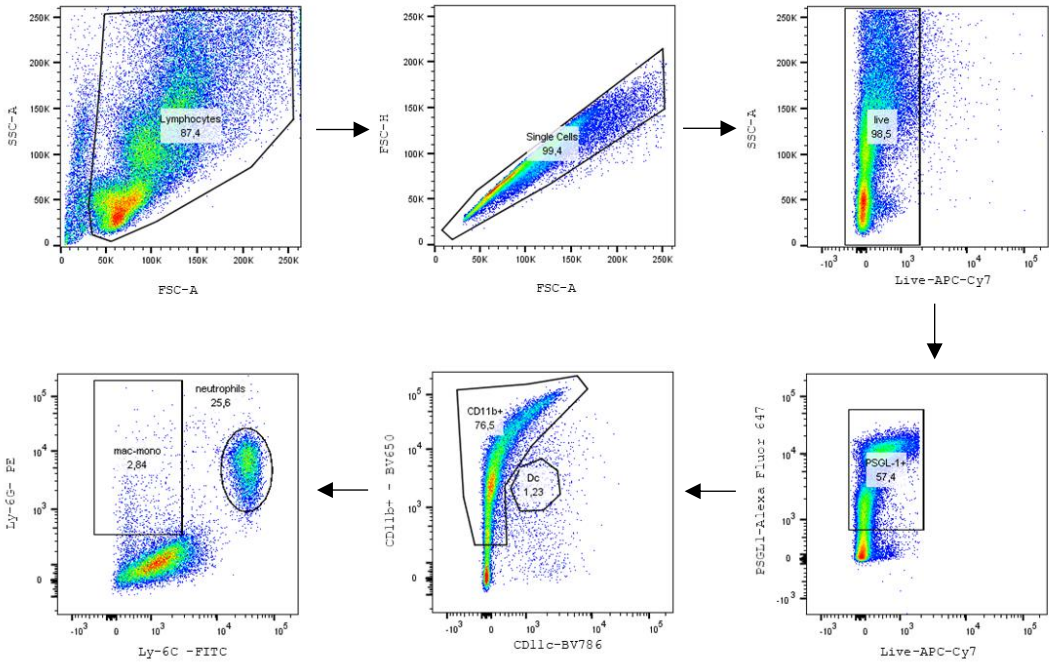

Figure 14. Gating strategy for the analysis of immune cells extracted from the peritoneal cavity. Cells were sorted by size and granularity and then selected to remove doublets. Live cells were selected using live dead staining. Live cells were then stained for PSGL-1. PSGL-1 positive cells were differentiated using CD11b and CD11c. CD11b positive cells were differentiated between neutrophils and monocyte/macrophage using Ly-6C and Ly-6G.

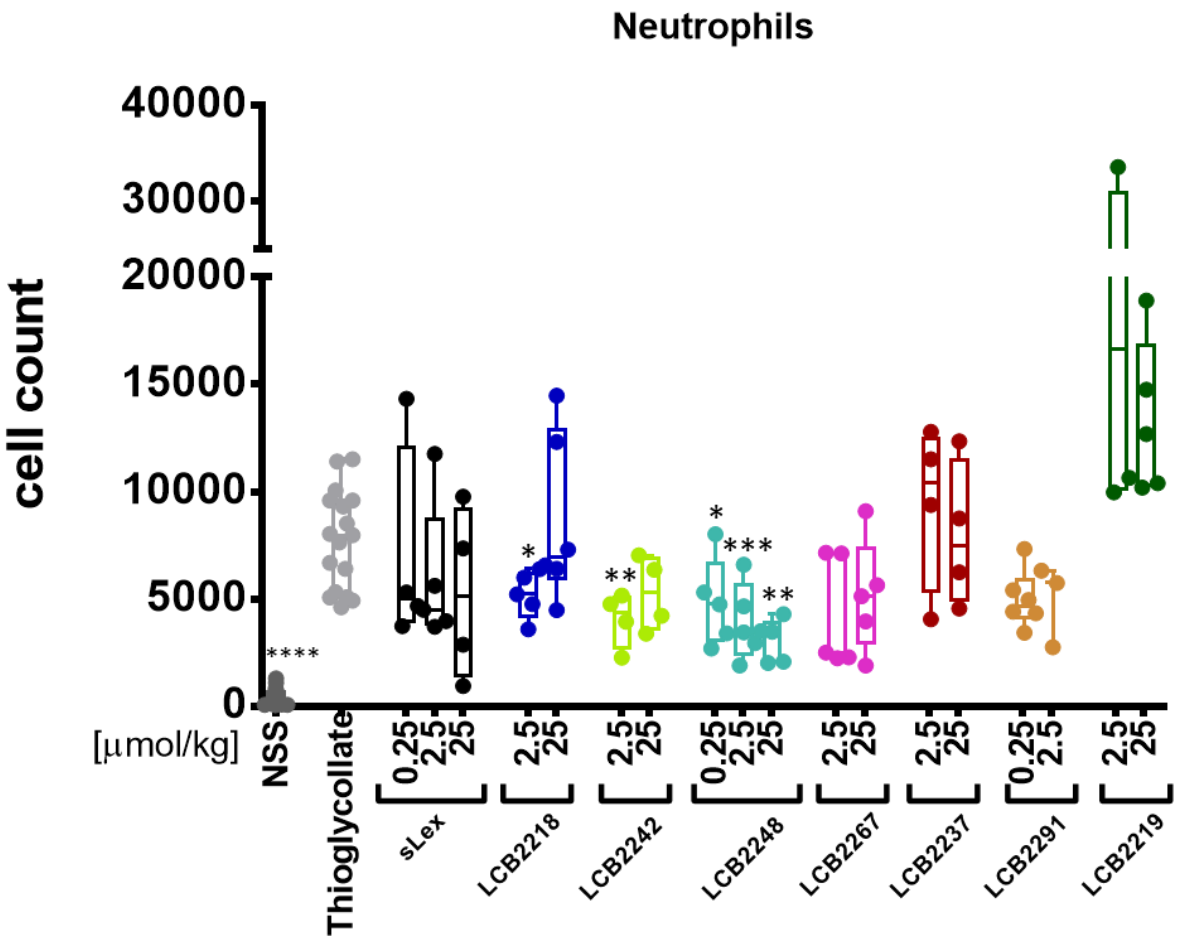
Neutrophils
cell count
40000
30000
20000
15000
10000
5000
0
[µmol/kg]
NSS
Thioglycollate
0.25
2.5
25
sLex
2.5
25
LCB2218
2.5
25
LCB2242
0.25
2.5
25
LCB2248
2.5
25
LCB2267
2.5
25
LCB2237
0.25
2.5
LCB2291
2.5
25
LCB2219
****
*
**
*
***
**

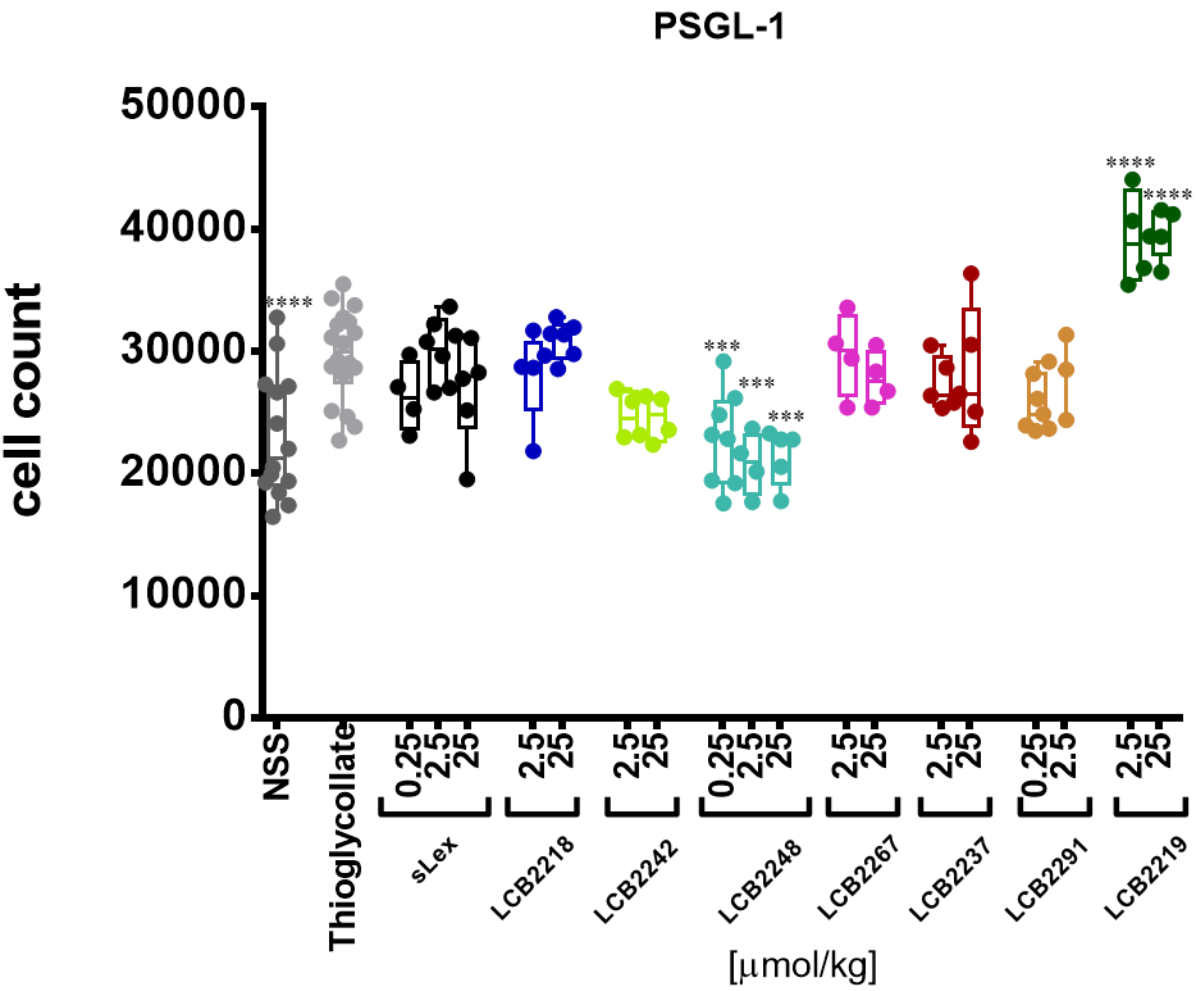

Figure 15. *In vivo* cell migration assay. Mice (n=3-5 for antagonists, n=17 for controls) were injected with 1mL 3% thioglycolate in the peritoneal cavity to stimulate cell recruitment. Mice were then treated with compounds at indicated doses through single IV injection. Cells were collected after 2hours from the cavity and identified using flow cytometry. PSLG-1 positive population was identified from total live cells. Neutrophils were identified as $CD11b^{+}$, $CD11c^{-}$, $Ly\text{-}6C^{+}$, $Ly\text{-}6G^{+}$. Significance was determined in comparison to thioglycolate stimulated mice using one-way ANOVA. *p<0.05, **p<0.001, ***p<0.0001, ****p<0.00001

7. Molecular basis of GATA5 in endothelial inflammation

7.1. Generation of GATA5 knockdown and overexpression cell lines

The second aim of this project is to determine if GATA5 plays a role in the selectin inflammatory response. As indicated earlier, mice lacking GATA5 have evidence of small vessel inflammation and endothelial cell dysregulation. In order to determine which genes are regulated by GATA5, we generated both a loss and gain of GATA5 function (Figure 16) using knockdown and overexpression in human dermal microvessel endothelial cells (HDMEC). HDMEC cells were selected as previous work in our group showed that they possessed the highest amount of GATA5 compared to other endothelial cell lines evaluated (unpublished results). Evaluated cell lines were the human coronary artery endothelial cells (HCAEC), human cardiac microvascular endothelial cells (HCMEC), human pulmonary microvascular endothelial cells (HPMEC), and HDMECs. The knockdown line showed a 60% reduction in the mRNA expression of GATA5. In the overexpression line, there was a 60-folds increase at the mRNA level, resulting in a 1.8-fold increase of GATA5 protein level (Figure 17). Transformed cell lines did not show any morphological changes or a change in cell survival allowing the identification of potential direct GATA5 downstream gene targets.

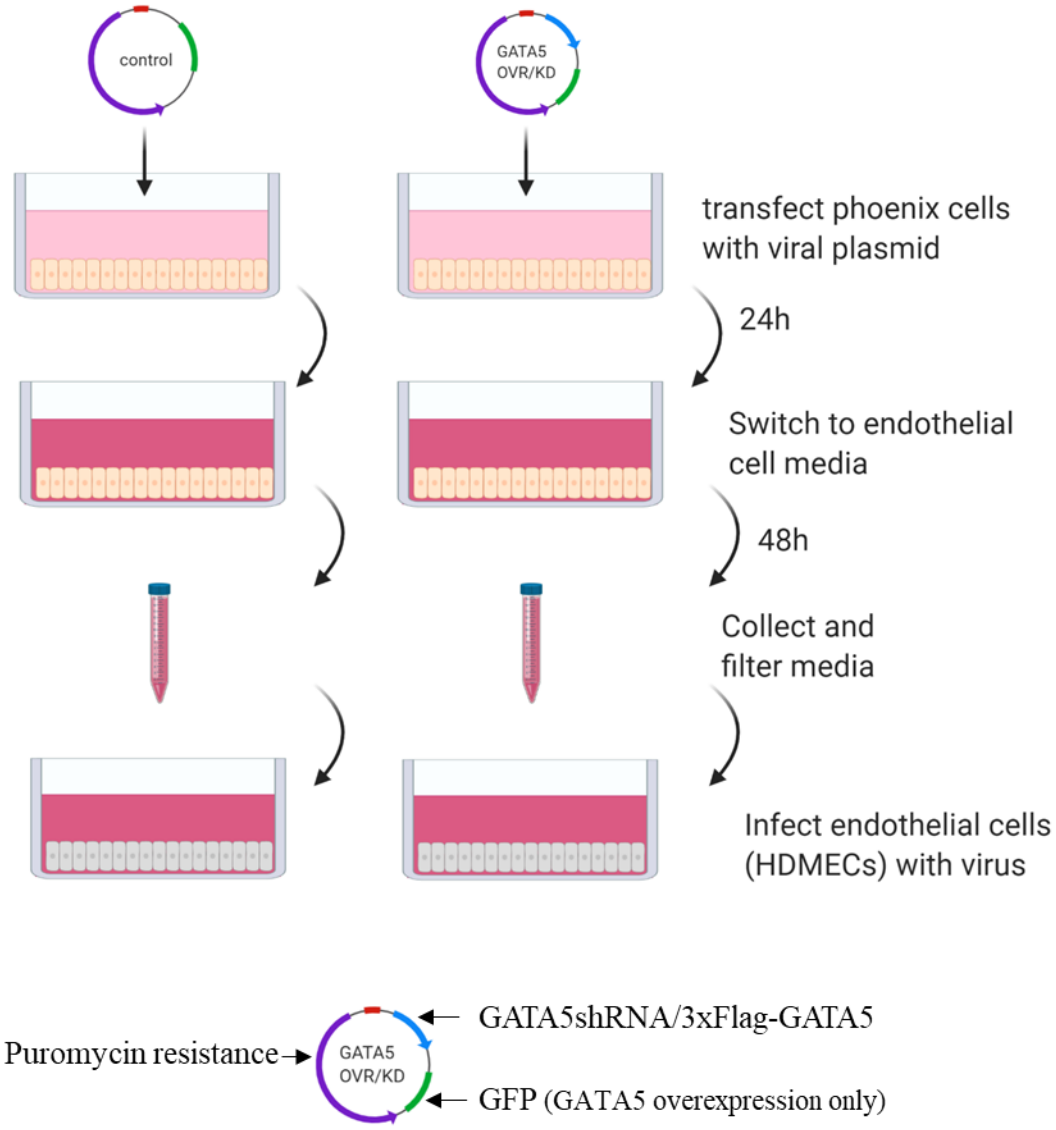

Figure 16. Schematic illustration of the generation of HDMEC cells with modified GATA5 expression. Phoenix cells were transfected 24h with either control or overexpression/knockdown plasmids as detailed in the Methods section. After 24h. cells were washed, and culture media was switched to endothelial culture media (MV2) for 48h. Virus was collected from endothelial media (MV2) and filtered to remove debris. HDMECs were infected with virus (retrovirus or lentivirus) containing media for 24h and treated with 2.5µg/mL Puromycin to select infected cells. Cells were maintained in 0.25µg/mL Puromycin after selection. Overexpressing cells were generated using MSCV-IRES-Neo-GFP plasmids. Knockdown cells were generated using pLNCX2 plasmid.

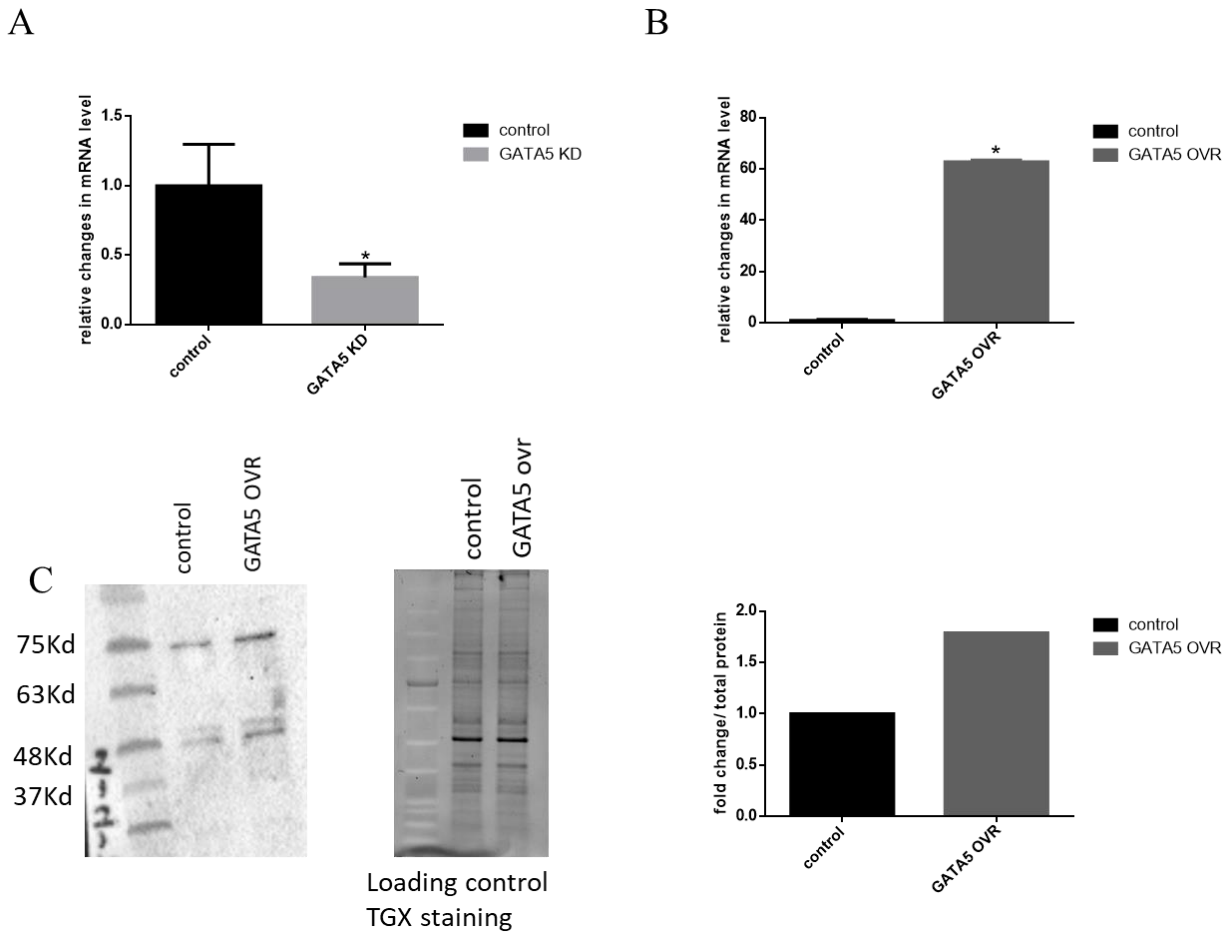

Figure 17. Confirmation of changes in GATA5 expression in infected HDMECs. **A)** QPCR determined relative GATA5 mRNA in HDMEC knockdown using lentivirus shRNA. Results are average of three separate experiment (±SEM) **B)** QPCR determined level of GATA5 mRNA in HDMEC overexpressing using retrovirus containing GATA5 vector. Results are average of three separate experiments (±SEM) **C)** Protein level of GATA5 overexpression (ovr) in HDMEC normalised over total protein (n=1). mRNA fold change levels were obtained in reference to S16 mRNA levels and normalised to control cells. Significance was determined using unpaired t-test *$p<0.05$

Previous work in our group, by Messoudi et al., included performing a microarray analysis using the GATA5 knockdown HDMEC (confirmed protein level at 0.44 fold relative to control) and control cells to evaluate GATA5-dependent genome-wide changes in gene expression[55]. The results showed broad gene expression changes including several pro-inflammatory genes, such as

ICAM1 and IL-6. I re-analysed the data with a focus on genes linked to inflammation and tight junction regulation using Ingenuity Pathway Analysis (Qiagen) [110]. The microarray chip (Mouse Gene 2.0) contained 222 inflammation-related genes that were evaluated out of which 58 (26%) were differentially regulated (Figure 18). The analysis also showed that the differentially expressed genes were linked to several pathways and pathologies including vascular lesion and vasculogenesis, familial vascular diseases, and cell migration (Figure 19). Inflammatory genes were then grouped as pro- or anti-inflammatory based on the literature. To determine if the genes identified could be directly influenced by GATA5, we examined their promoters (-1000bp from transcriptional start site) for putative GATA binding sites (Tables 2, 3, 4) using Genomatix (Genomatix Software GmnH)[111]. We found that multiple pro-inflammatory genes were upregulated, while the anti-inflammatory genes were suppressed, indicating that the loss of GATA5 causes the endothelial cells to be in a pro-inflamed state. Changes in transcript levels of several pro-/anti-inflammatory and tight junction genes were further confirmed using QPCR analysis of RNA from the GATA5 knockdown and overexpression cell lines (Figure 20).

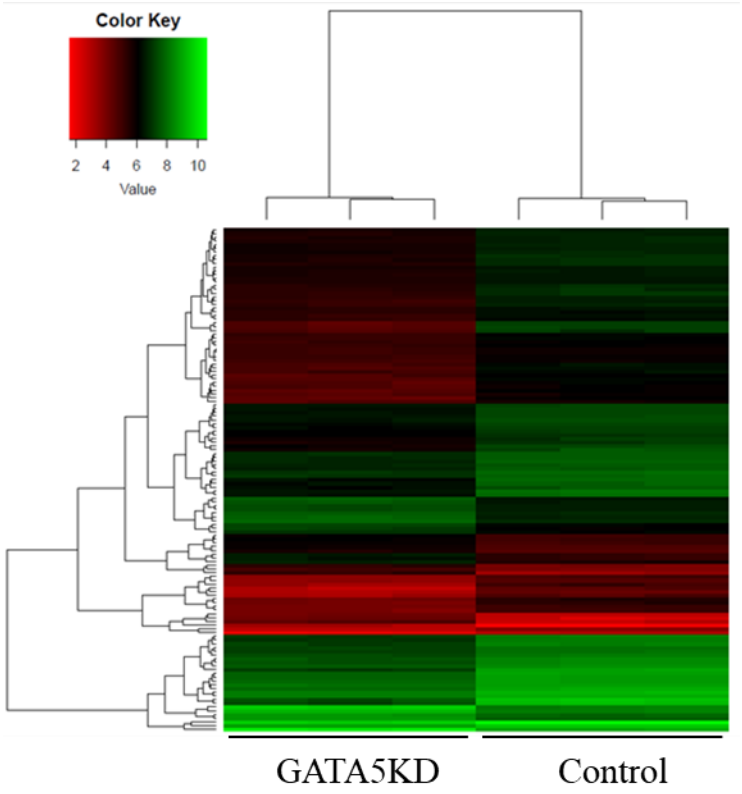

Figure 18 . Heatmap of genes linked to inflammation as determined by microarray analysis of GATA5 KD and control HDMECs.

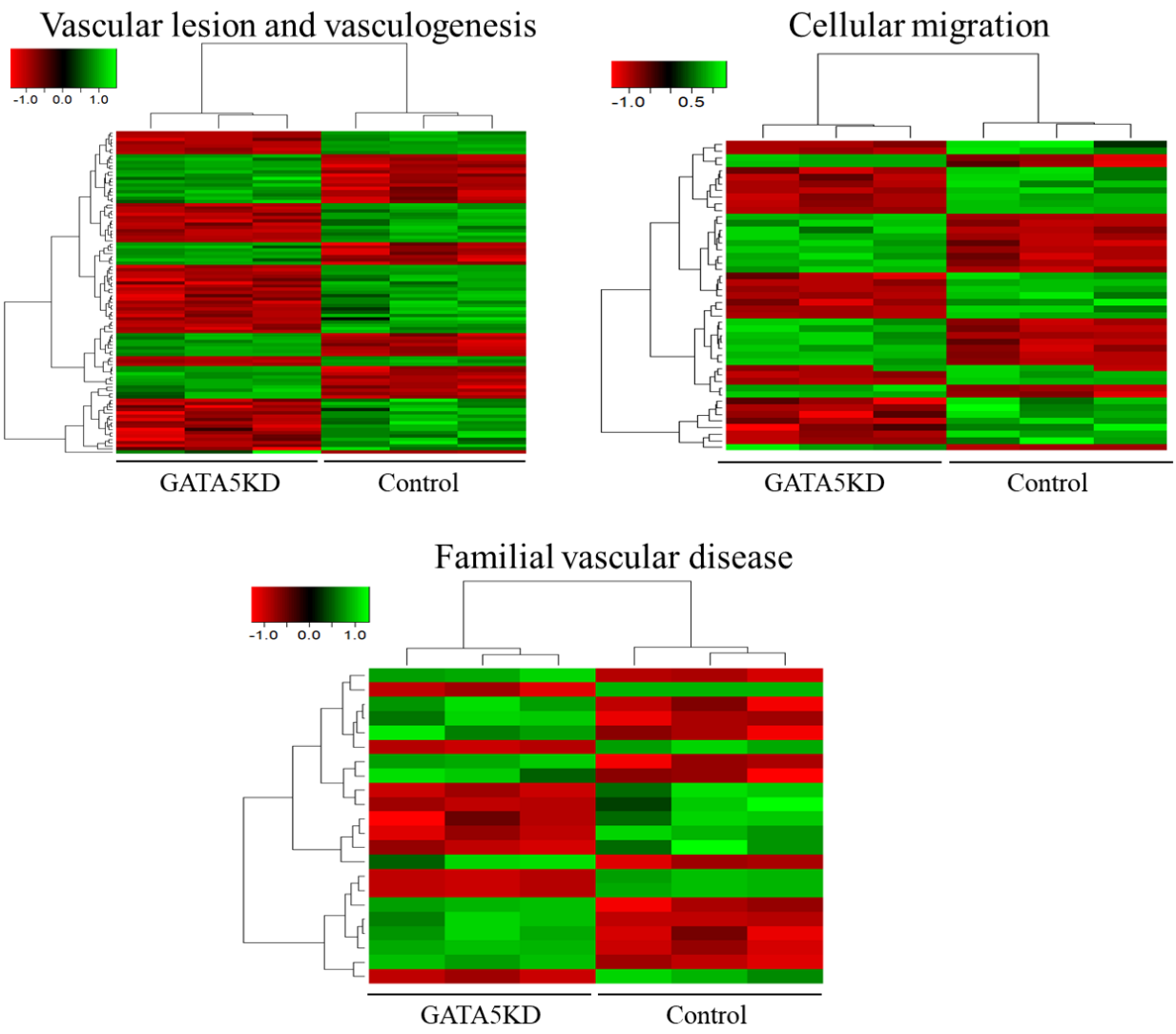

Figure 19. Heatmaps of differentially expressed genes in HDMEC GATA5 KD involved in vascular lesion and vasculogenesis, cellular migration and familial vascular disease.

Table 4. Pro-inflammatory genes significantly ($p<0.05$) changed in GATA5 KD HDMEC microarray. Position of GATA, NF-kB, STAT, SMAD and NFAT binding elements in the promoter (-1000bp) was determined using in silico analysis. N= no region on promoter. GATA, NFκB, STAT, SMAD and NFAT indicate location of binding site in promoter.

gene	name	fold change (KD vs WT)	GATA	NFkB	STAT	SMAD	NFAT
PLAT	plasminogen activator, Tissue Type	2.44	N	-966 308	-36 -34	-660	-796 -792 -787 -652 -29
COL1A2	collagen, type I, alpha 2	2.36	-497	-795	-926 -640 -240	-992 -777 -515 -450 -262	-321 -243 -50 -41
ITGB8	integrin, beta 8	2.09	N	-916 -792 -791 -104	-920 -565 -564 -353 -351	-306 -122	-358
MIR612	microRNA 612	1.78	-574	-888 -791 -726	-882 -612 -610 -482 448	N	-676 -595 -417 -415
MIR154	microRNA154	1.64	-404	-283 -57	-635 -518 -506 -504 -352 -350 -251 -53 -51	-170	-499 -328 -217
IL6	interleukin 6	1.62	-944 -28	-699 -420 -14 -14	N	-829 -244 -125	-421 -143 -83 -15
PKD1	polycystic kidney disease 1 (autosomal dominant)	1.53	N	-239 -185	-806 -683 -682	-879 -233	-680 -634 -632
ICAM1	intercellular adhesion molecule 1	1.52	-53	-314 -238	-468 -287 -286 -203	-688	-867
PELI1	pellino E3 ubiquitin protein ligase 1	1.5	-615 -561 -402	-299	-518 -516 -447	-359	-961 -877 -875 -511 -200 -195

ANXA3	annexin A3	0.67	-906 -676 -626 -593 -259 -243 -34	N	-743 -742 -601 -600 -423 -308	N	-265
REL	v-rel avian reticuloendotheliosis viral oncogene homolog	0.66	-952 -846 802	-574 -573 -274	-915 -913 -820	-981 -264	-596 -594
MYL9	myosin, light chain 9, regulatory	0.65	N	-571 -394 -281	-767 -466	-606	N
ALCAM	activated leukocyte cell adhesion molecule	0.64	-343	-852 -852 -643 298	-987 -985 -750 319	-280 -208	-597 -595 -564 -37
ADK	adenosine kinase	0.63	-755	-313	-674 -673	-39	-811 -726 -671 -523 -276
MYLK	myosin light chain kinase	0.6	-799 -503 -335	-962 -962	N	N	N
BIRC5	baculoviral IAP repeat contining 5	0.59	-862 -638	-662 -662	-588 -129 -127	-491 -442	-581
BMX	BMX non-receptor tyrosine kinase	0.58	-942 -677 -634 -585 -567 -415	-79	-915 -516 -359	-252 -103	-830 -741 -739 -644 -543 -538 -455 -450 -411 -264
PDE8A	phosphodiesterase 8A	0.57	N	-932 -442 -442 -354	-913 -125 -124	-579 -573 -496 -289 -76	-933 -931 -772 -770 -355
TNFRSF1B	TNF receptor superfamily member 1B	0.55	-205	N	-359	-741 -729 -109	-328 -326
IL1R1	interleukine 1 receptor, type I	0.54	-709 -641	-930 -930 -38 -38	-523 -521	-733	-512
IL31RA	interleukine 31 receptor A	0.54	-823 -397	-955	-817 -769 -552 -550	-517	-682 -218

Table 5. Anti-inflammatory genes significantly ($p<0.05$) changed in GATA5 KD HDMEC microarray. Position of GATA, NF-kB, STAT, SMAD and NFAT binding elements in the promoter (-1000bp) was determined using in silico analysis. N= no region on promoter. GATA, NFκB, STAT, SMAD and NFAT indicate location of binding site in promoter.

gene	name	fold change (KD vs WT)	GATA	NFkB	STAT	SMAD	NFAT
ABCA1	ATP-binding cassette, sub-family A (ABC1), member 1	2.00	-843 -743 -541	-563 -563	-326 -310 -279 -277	-427	-439 -352 -339 -337
TUSC2	tumor supressor candidate 2	1.63	-958 -939 -653	-83	-418	-694 -516 -290	-157
HBEGF	heparin-binding EGF-like growth factor	1.55	-972 -937 -477	-21	-866 -625 -463 -243 -62	N	-868 -859 -692 -665
ADA	adenosine deaminase	1.52	-926 -910	-637	-793 -759 -345 -88 -86	-736 -529 -242 -49	-877 -797 -638
TERC	telomerase RNA component	0.67	-315	N	-395 -308 -307 -178 -176	-425 -269	-574
NQO2	NAD(P)H dehydrogenase, quinone 2	0.66	-881 -759	-948 -471 -470	-954 -924 -906 -904 -808 -410 -408	N	-947 -940 -818 -422 -420
AHR	aryl hydrocarbon receptor	0.65	-957 -899 -891 -847 -683 -462	-405	N	N	-509 -507 -404
STAC	SH3 and cysteine rich domain	0.64	-528 -509 -397 -381	-770 -339 -338	-809 -808 -98	-667	-762
RRM2	ribonucleotide reductase M2	0.62	-974	-269 -268 -75 -74 -51 -50 -17	-967 -965 -953 -951 -712 -710 -362	-175	-708 -706 -704 -369
MIR146A	microRNA 146a	0.62	N	-454	-494 -104	-351 -167 -114	-677 501
SPHK1	sphingosine kinase 1	0.62	N	-842 -800 -183	-62	-897 -585	-775 -663 -345 -206 -204 -83 -64 -55
IL1A	interleukin 1, alpha	0.60	-188	N	-667 -368	N	-942 -770 -185
NQO1	NAD(P)H dehydrogenase, quinone 1	0.60	-283	-741 -479	N	N	-789 -664

IGFBP1	insulin-like growth factor binding protein 1	0.60	-708 -590 -353	-363	-688 -686 -656 -655 -640 -638	N	-364 -362 -305
TNFAIP3	tumor necrosis factor, alpha-induced protein 3	0.58	-832 -800	-578 -456 -198 -197 -175	N	-462 -385	-281 -257
CLU	clusterin	0.58	-482 -248	-184	-621 -593 -322 -161	-958 -87	-809 -215 -168
HSD11B1	hydroxysteroid (11-beta) dehydrogenase 1	0.56	-888	-807 -581	-743 -741 -519 -517 -467	N	N
SCD	stearoyl-CoA desaturase (delta-9-desaturase)	0.55	-946 -395	-661 -660 -482 -482	-866 -865 -354 -353	-682	-940 -767 -756 -358

Table 6. Tight junction genes significantly ($p<0.05$) changed in GATA5 KD HDMEC microarray. Position of GATA, NF-kB, STAT, SMAD and NFAT binding elements in the promoter (-1000bp) was determined using in silico analysis. N= no region on promoter. GATA, NFκB, STAT, SMAD and NFAT indicate location of binding site in promoter.

gene	name	fold change (KD vs WT)	GATA	NFkB	STAT	SMAD	NFAT
CLDN1	claudin 1	2.5	-821 -764 -645 -270	-119	N	-903 -553	-975 -604 -414
CLDN2	claudin 2	0.82	-855 -36	N	-412	-55	N
MYL9	myosin, light chain 9, regulatory	0.64	N	-571 -394 -281	-767 -466	-606	N
MYH10	myosin, heavy chain 10, non-muscle	0.62	N	-9	-159	-878 -244	-101 -96
F2RL2	coagulation factor II (thrombin) receptor-like 2	0.61	N	-578	-982 -980	N	-391 -345 -39
MYLK	myosin light chain kinase	0.6	-799 -503 -335	-962 -962	N	N	N
PRKAR2B	protein kinase, cAMP-dependent, regulatory, type II beta	0.6	-938 -886 -881 -600 -481 -369	-978 -978 -179	N	-116	-663 -342
PRKACB	protein kinase, cAMP-dependent catalytic, beta	0.56	-962 -544 -374 -238 -226 -88 -47	N	-933 -932 -644 -643 -592	-139	-926 -69 -64
TNFRSF1B	tumor necrosis factor receptor superfamily, member 1B	0.55	-205	N	-359	-741 -729 -109	-328 -326
TJP1	tight junction protein 1	0.5	-957 -953 -185	-321 -118	-826	N	-414 -409 -351 -240
OCLN	occludin	0.48	-845 -844 -823 -689	N	-954 -952 -569 -370 -164 -123 -121	N	-955 -572 -567 -171 -173 -69 -24
PRKCI	protein kinase C, iota	0.42	-792 -679	N	-538 -439 -437 -313 -287	N	-583 -444 -407 -405

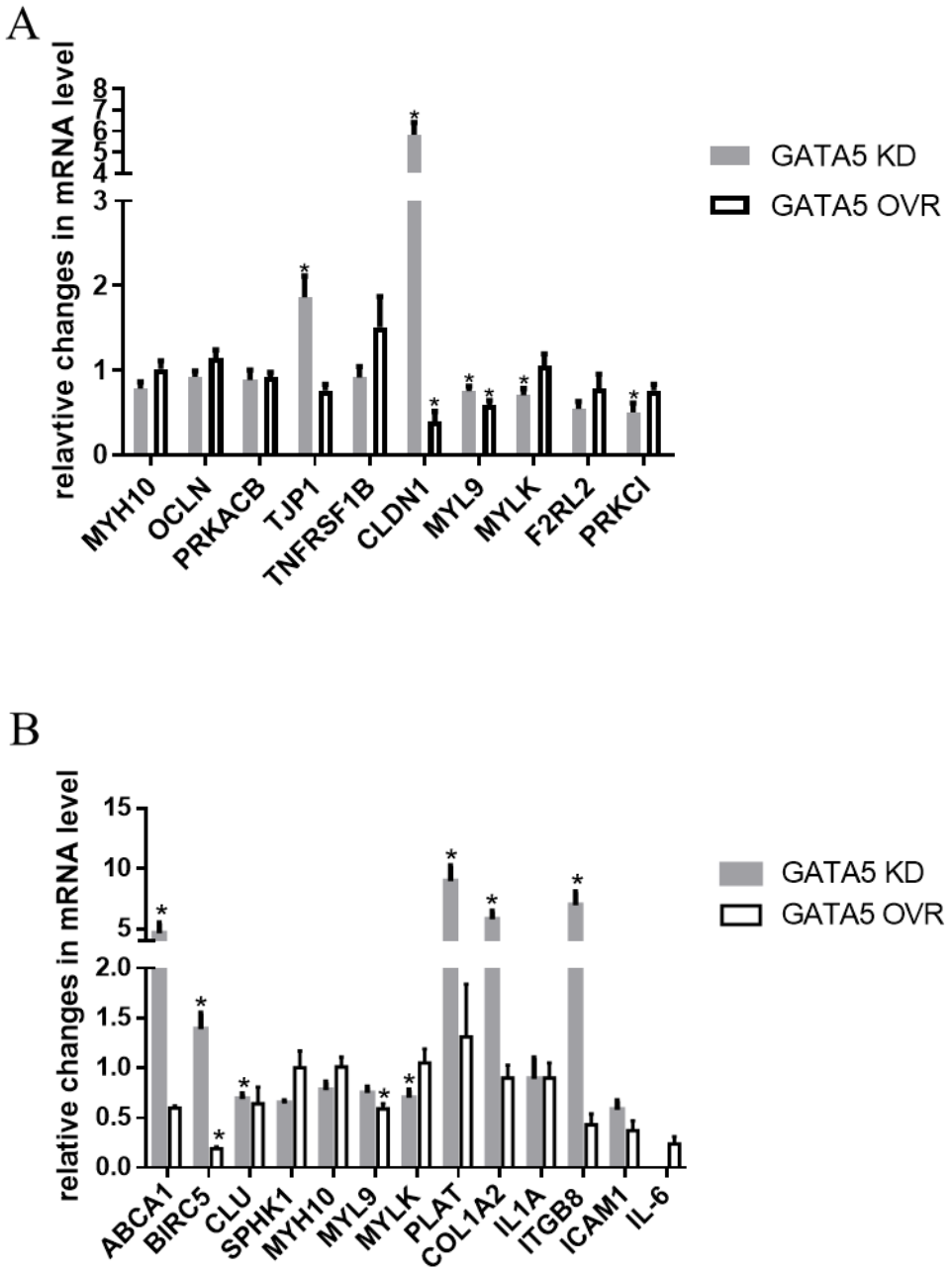

Figure 20. Effects of changes in GATA5 expression on transcript levels in HDMEC. **A)** mRNA levels of genes associated with tight junction in HDMEC with GATA5 knockdown and overexpression. **B)** mRNA levels of genes associated with inflammation in HDMEC GATA5 knockdown and overexpression. Results are represented as the average of three separate experiment ±SEM. mRNA levels were divided by S16 mRNA levels and normalised to control HDMEC cells. Statistical significance was determined using unpaired t-test. *$p<0.05$

Expression of three genes was significantly altered in both the HDMECs with a GATA5 knockdown and overexpression; namely, BIRC5 (survivin), CLDN1 (claudin 1) and MYL9 (myosin light chain 9). Expression of Survivin, a known anti-apoptosis gene, is known to be increased during inflammation[112]. CLDN1 is an important component of the tight junction regulation[113]. Patients with inflammatory bowel disease have been found to have an increased expression of CLDN1[114]. Myl9 has been shown to help the migration of activated T-cells in the blood vessels in inflamed lungs[115]. CLDN1 and BIRC5 were changed in opposite direction as a result of the changed GATA5 expression, while MYL9 expression was decreased in both conditions. Several genes such as ICAM1, IL-6, and ITGB8 showed a decreased trend although it didn't reach statistical significance. CLDN1 is an important player in cell-cell adhesion of endothelial cells. The adhesion of the endothelial cells affects the ability of immune cells to extravasate and control vascular leakage. CLDN1 possesses four GATA binding sites in its promoter, indicating a great potential to be directly controlled by GATA5. The expression level of ICAM1 was not increased in the qPCR, contrary to the results obtained in the microarray. The selectin levels were not changed by decreased GATA5 levels in either the microarray or the QPCR assays. In the overexpression cells, there appears to be a trend to decrease the expression of the selectin that did not reach statistical significance.

To further evaluate changes in the endothelial wall of the Gata5 null mice and establish whether they represent a novel chronic inflammation model, we examined gene expression changes in endothelial cells of Gata5 null mice.

7.2. Expression of inflammatory and cellular adhesion genes in Gata5$^{-/-}$ mice

Next, we checked whether the gene expression changes obtained in the human endothelial cell lines were also present in endothelial cells from the Gata5$^{-/-}$ mice. Gene expression was measured in endothelial cells extracted from the lungs of the Gata5 null and control mice (Figure 21 A, B). As stated earlier and shown in Figure 21C, GATA5 is present in human pulmonary microvascular endothelial cells (HPMEC) albeit at lower relative levels to HDMEC. However, the endothelial cells are abundant in the highly vascularised lungs, and several inflammatory diseases are known to impact the lungs.

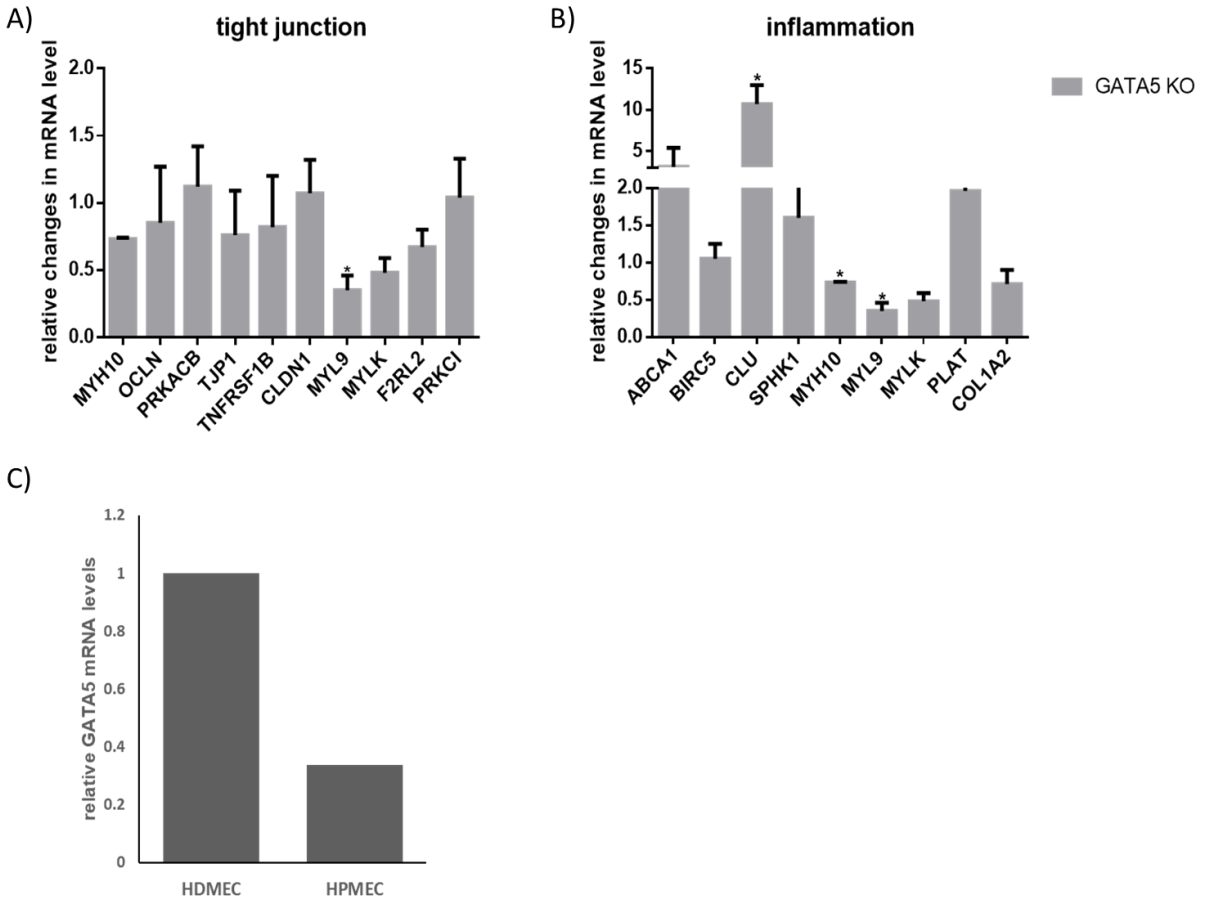

Figure 21. Changes in mRNA levels in lung derived endothelial cells from female 60-day old Gata5 null mice. **A)** genes associated with tight junction and **B)** genes associated with

inflammation. mRNA levels were divided by S16 mRNA levels and normalised to WT mice (n=3). Statistical difference was determined using unpaired t-test. *p<0.05 **C)** GATA5 expression levels in human dermal and pulmonary microvascular endothelial cells (n=1)

Three genes showed a statistically significant altered expression in the Gata5 null mice; a decrease of Myl9 and myosin heavy chain 10 (Myh10), while clusterin (Clu) increased. The loss of Myh10 has been linked to chronic obstructive pulmonary disease (COPD). COPD is characterised by airway inflammation and the destruction of the extracellular matrix. The destruction of the extracellular matrix (ECM) increases tissue stiffness that modulates the cellular adhesion[116]. Clusterin is known to be expressed following an inflammatory stimulus such as TNFα. Clusterin is also known to be involved in the regulation of NF-κB a well-known regulator of inflammation[117]. The expression of ICAM1 was not altered in the lung endothelial cells. The expression of E and P selectin were decreased but did not reach statistical significance. The genes involved in tight junctions, Tjp1 (increased 1.8 fold in GATA5 KD HDMECs), Cldn1 (increased 5 fold in GATA5 KD and reduced 0.4 fold in GATA5 OVR HDMECs) and Ocln (not changed in GATA5 altered HDMECs) were not changed in the lung endothelial cells from Gata5 null mice suggesting that there is no increased vascular permeability in their lungs at a basal level.

7.3. TNFα stimulation in HDMEC and GATA5 knockdown HDMEC

After measuring the expression of inflammatory and tight junction genes at the basal level, we evaluated whether GATA5 levels alter the transcriptional response to TNFα treatment in HDMECs (Figure 22). TNFα is known to activate the expression of cellular adhesion molecules and the inflammatory response of cells by increasing the expression of E-selectin, ICAM-1, and VCAM-1[118]. HDMECs were treated with TNFα for 3h, and QPCR analysis revealed changes in the

expression of several genes. The expression of several genes is similar between the control and GATA5 KD cells including CLDN1, MYL9, and E-selectin. The expression of E-selectin is upregulated in both the control and KD cells but is much less stimulated in the HD HDMECs. Other genes showed differential expression between the control and KD once treated with TNFα, these include: OCLN, TNFRSF1B, ABCA1, PLAT, COL1A2, and SPHK1. The expression of ICAM1 was not altered in this short treatment; its expression has been found to be increased in vascular cells treated with TNFα but only after a 16-24h period.

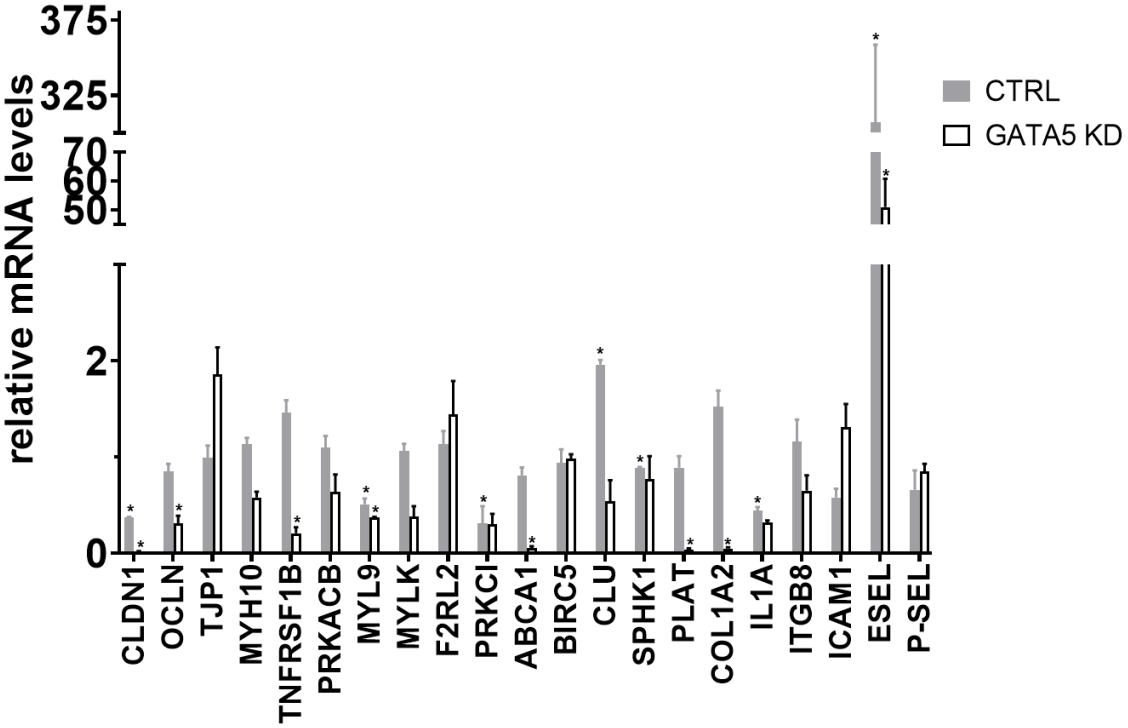

Figure 22. mRNA response to TNFα treatment over non-stimulated control and GATA5 KD HDMECs. Fold changes were obtained by dividing treated cells over non-treated cells. mRNA levels were divided by S16 mRNA levels and normalised to respective control cells. Statistical significance was determined using unpaired t-test. *$p<0.05$

7.4. Role of GATA5 in selectin regulation and activity

As shown before, the loss of GATA5 does not lead to a direct effect on the regulation of E- and P-selectin expression. While there is no direct effect on the transcript level of the selectins, it is still possible that there is an effect on the ability of the endothelial cells to bind to circulating leukocytes. To evaluate this, we performed a cell-cell adhesion assay using the GATA5 knockdown cells without TNFα stimulation. TNFα stimulation was not added to evaluate the increase in cellular adhesion at baseline caused by a 50% decrease in GATA5. We found that decreased GATA5 levels did not increase the adhesion of the HL-60 to the modified HDMEC (Figure 23). This cellular adhesion assay is performed in a static environment. However, as previously mentioned the binding affinities of inflammatory cellular adhesion proteins are greatly increased as a result of the blood flow (such as ICAM-1/LFA-1). The role of GATA5 on cellular adhesion may only be evident under flow or in stimulated conditions.

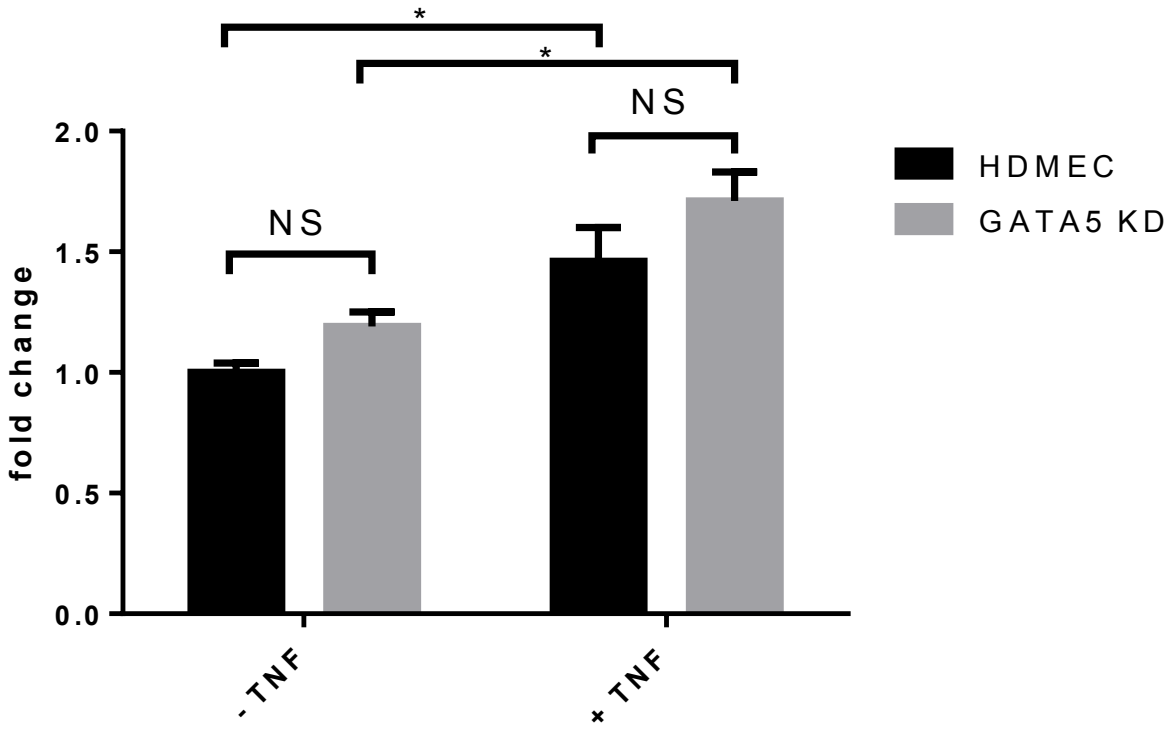

Figure 23. Cell-Cell binding assay in WT and GATA5 KD HDMEC. Cell-cell static binding assays of HDMEC and LeukoTracker® labelled HL-60s (1h). Cells were lysed 5min and fluorescence was measured using Synergy H1 plate reader to determine binding. Results are the mean of three separate experiments (±SEM) normalised to individual internal controls.

Discussion

Inflammation is an important factor in several diseases including infections, thrombosis, anemia, cardiovascular diseases, and cancer[11,19,20]. Its role in these various diseases makes it a major burden on the healthcare system. There are several diseases for which there are no effective anti-inflammatory treatments[119]. The current and previous standard treatments, using corticosteroids and NSAIDS respectively, are associated with multiple secondary effects such as hepatic injury, platelet inhibition and cardiovascular toxicity[24,28]. The development of new anti-inflammatory treatments is therefore required.

An important player in the cellular recruitment inflammatory process is the selectin family. These are the first proteins to initiate the recruitment of leukocytes to the vascular wall[40]. The interaction between the leukocytes and the selectins also increases the binding of leukocytes to integrins, for example, the interaction between LFA-1 and ICAM1[44,75]. The selectins, E and P, have been shown to have a role in various inflammatory diseases, including thrombosis and sickle cell anemia[11,15]. They have also been implicated in the ability of cancer metastasis to migrate to other tissues[76]. Given the important role of the selectins in inflammation, they have become an interesting target for the development of new anti-inflammatory treatments. This is what inspired the Guindon laboratory at the IRCM to synthesize novel small molecules that inhibit the selectins. As mentioned in the introduction, there have been previous small molecules synthesized to inhibit the selectins, TBC-1269 and Rivipansel. However, these molecules were only able to inhibit E-selectin effectively[95,97]. Their ability to only inhibit E-selectin may be a factor that lead to their failure to pass through clinical trials. Based on the work done for this thesis, the novel molecules

synthesized by the Guindon group which I tested, are the only known inhibitors that can interact with both E and P-selectin.

Two categories of molecules were evaluated. The first category of molecules contains an anionic side chain on a sLex core. The second category aimed to lock the carboxylic acid into the bioactive configuration. The lead candidates in each category were then used to generate a combined analogue whose binding affinity could be higher than the individual compounds as there would be an increase in the binding for both binding sites. We first screened the compounds in an *in vitro* assay using surface plasmon resonance (SPR) to determine their ability to bind directly to the selectins. This assay allows us to predict the ability of our compounds to inhibit the binding of leukocytes bound directly to the selectins. Molecules from the first category, the anionic side chains, consist of LCB 2204, 2236, 2205, 2237, 2219, 2238, and 2218. The second category, the bicyclic cores, consists of LCB 2248, 2242, 2294, 2251, 2298, 2299, and 2292. Finally, the combined molecule, LCB 2291, is the combination of the core of LCB 2248 and the side chain of LCB 2218. LCB 110 and LCB 2300 are molecules from the first generation previously evaluated[98]. LCB 2300 is a modified version of LCB 111 so that it could be dissolved in a saline solution more easily.

For the anionic side chain molecules, the SPR assay showed that they all have a higher affinity than the molecules from the first-generation (LCB 111, LCB 2300) to P-selectin or any positively charged region. All the side chains possess a group that could bind to the sulfated tyrosine pocket of P-selectin. While all the side chain analogues show a higher affinity to P-selectin

the two antagonists that show the best inhibition are LCB 2218 and LCB 2219. Their increased affinity can be explained by the length of the side chain. LCB 2218 and LCB 2219 possess longer side chains that may be able to interact more with the sulfated tyrosines. Both LCB 2218 and LCB 2219 also show better binding against E-selectin. As E-selectin does not possess the sulfated tyrosine pocket the improved binding was unexpected. For some of the antagonists, the side chains were attached in either the R and S position on the original core. This allows us to evaluate if the stereochemistry of the side chains could influence the binding affinity. Only LCB 2237 (R) shows an improved binding compared to LCB 2205 (S). All the other molecules show no difference in their binding ability between the R and S configuration, suggesting that the stereochemistry does not play an important role in the binding affinity.

Molecules possessing the bicyclic core either show a strong binding affinity to both P-Selectin and E-Selectin or no binding. LCB 2242 does not possess a benzoate at the C6 position and showed no binding. LCB 2248 shows a 2 folds increase in the affinity for P-selectin and a 5 fold increase in the binding affinity with E-selectin compared to the previous generation (LCB 110). LCB 2298 shows a 7 fold increase in the affinity with P-selectin and a 2 fold increased affinity with E-selectin relative to the binding affinity of LCB 110. These results show that the amine group on the C9 position of the carboxylic acid has a strong affinity with E-selectin while the carboxyl group allows a strong affinity with P-selectin.

As the SPR assays are *in vitro* and do not necessarily reflect what happens *in vivo,* molecules were then evaluated progressively in cell-based assays to resemble more and more blood vessels and their environment.

The cell-selectin assay allows us to determine the effect of our molecules on the interaction of selectins and immune cells. Using this assay, LCB 2237 has been found to be the best inhibitor against the binding to P-selectin, LCB 2219 is the best inhibitor against E-selectin from the anionic side chain category. LCB 2237 has an IC50 (0.04 μM) 100 times smaller than the IC50 of sLex (1.2 uM), the natural ligand, against P-selectin. The IC50 of LCB 2219 (0.1nM) is 1000 times lower than the IC50 of sLex (4uM) against E-Selectin. In the second category LCB 2248, 2267, and 2225 show similar inhibitory capacities against P-selectin. LCB 2248 and 2267 are similar molecules except for the group in C9 of the bicyclic being either in axial or in equatorial position respectively. LCB2242 was surprisingly the best inhibitor against E-selectin reaching a maximum inhibition of 84% and is the only compound that has a significant increased inhibitory potential over sLex. The IC50 of LCB 2242 (0.03 μM) is much lower than the IC50 of sLex (4mM) on E-Selectin. LCB 2291 did not show an improved inhibitory activity in the cell-selectin reaching a maximal inhibition of 60% against both selectins. The individual compounds that were combined to obtain LCB 2291, LCB 2248, and LCB2218, have a better inhibitory potential individually. However, the selectins are not the only proteins expressed at the surface of the endothelial cells in blood vessels.

Our second cellular based assay was the cell-cell binding assay. In this assay, human dermal microvascular endothelial cells were used to simulate the endothelial layer of blood vessels. The presence of endothelial cells allows the potential changes in activity caused by other cellular adhesion proteins to be evaluated and are consistent with the *in vitro* binding assay. Our results show that LCB 2219 has the highest inhibitory potential of the antagonists evaluated. The cellular assays described above are static. In the absence of flow the affinity of the interaction between selectins and their ligands are week (K_{off} high). Thus, the importance of the *in vivo* assays.

Finally, candidates were evaluated in an *in vivo* model. The *in vivo* model using mice allows us to evaluate how our antagonists would interact in the vessels with all of the flow conditions and potential protein partner present. It allows for the influence of other cellular adhesion molecules as well as the effects caused by the shear stress from the blood flow. Antagonists that showed good activity in the previous assays were evaluated in the peritoneal cavity mouse assay. In this assay, we identified the various immune cell populations that migrated to the peritoneal cavity two hours following a thioglycolate stimulus. Using various cell surface markers, we were able to identify the PSGL-1 positive population as well as the neutrophil population. Cells were given only two hours to migrate allow us to measure only the cells that migrated as they did not have enough time to divide and grow at the site of injury. Neutrophils population was evaluated as neutrophils are the first immune cells to be recruited in the inflammatory response[2]. Only one of the evaluated antagonists, LCB 2248, was able to reduce the number of neutrophils and PSLG-1 positive cells that migrated. Other antagonists, LCB 2218, 2242, and 2291, were only able to reduce the number of neutrophils at the lowest dose tested. LCB 2219 surprisingly lead to an increase in the number of neutrophils as well as the number of PSGL-

1 positive cells that migrated. This suggests that some of our molecules may also act as agonists or partial agonists of the selectins found on the endothelial cells and on the platelets. The agonist effect could explain why several of our molecules do not reduce the number of migrated cells at the higher dose.

The combination of these assays allowed us to determine that LCB 2218 was the most effective inhibitor in the anionic side chain category while LCB 2248 was the most effective bicyclic. The two modifications were then combined to generate LCB 2291 in the hopes the combination would create an even more effective inhibitor. Unfortunately, the combined modifications did not improve the ability of the inhibitor to reduce the number of migrating leukocytes. The addition of the LCB 2218 side chain to the bicyclic core of LCB 2248 did not lead to an increase in the inhibitory action of our compounds. Leading us to conclude that LCB 2248 is the most effective of our antagonist. We could next examine the possibility of attaching a different side chain that could inhibit another receptor involved in leukocyte recruitment, such as a CXCR4 inhibitors[120,121]. These inhibitors, synthesised in Dr Guindon's laboratory, are the only known antagonists able to block the binding to both E-selectin and P-selectin. The ability to block both is crucial as they both play an important role in various inflammatory diseases. Future steps to develop new antagonists are to evaluate their ability to inhibit cellular adhesion in a cellular flow dependant assay. In this assay, endothelial cells are treated to specifically express E or P-selectin followed by the addition of leukocytes in a flow. This will allow the affinity to the selectins to be higher (lower K_{off}), which could explain the difference observed between our static assay and our *in vivo* assay. Furthermore, the antagonist could be evaluated in an intravital microscopy model *in vivo,* in which a small window is surgically implanted in mice allowing the visualisation

of capillaries and the cells circulating in them. This assay allows to measure the speed at which tagged leukocytes circulate in the blood vessels.

The regulation of the homeostasis of endothelial cells is an important factor in the inflammatory response[36]. Endothelial cells activate or repress the expression of their genes as a result of the various extracellular signals that they receive. Identifying the genes that play a role in the regulation of endothelial homeostasis is therefore very important. A candidate regulator of endothelial cell response to inflammation is transcription factor GATA5. As indicated earlier, GATA5 has been shown to play an important role in the differentiation of cardiac endothelial cells, and loss of GATA5 has been linked to the development of a bicuspid aortic valve, a process involving endothelial cells[53,54]. More recently work done in the Nemer laboratory has shown GATA5 to be involved in endothelial cell homeostasis and its loss lead to the development of hypertension, a known inflammatory disease[55].

The second aim of my project was to evaluate the role of GATA5 in inflammation and more specifically its role in the selectin-dependent response. We first evaluated if decreased levels of GATA5 led to a pro-inflammatory response in endothelial cells. Previous work in the Nemer lab generated endothelial cells with GATA5 knockdown using human dermal microvascular cells (HDMEC). Those cells were used to identify, using RNA microarray, changes in gene expression attributed to loss of GATA5 function. The data was further analyzed to identify the inflammatory and cellular adhesion genes whose expression was modified. The analysis indicated a decrease in the expression of several anti-inflammatory genes (IL1A, SPHK1, CLU). The analysis also

showed a decrease in most of the genes associated with tight junctions (CLDN2, TJP1, OCLN). The combination of the decreased levels of anti-inflammatory genes and the decrease of tight junction genes indicate that the cells would result in an increased vascular permeability. Genes whose expression was altered in the microarray results were then validated by QPCR. Inflammatory genes that were validated by QPCR include survivin (BIRC5), PLAT (plasminogen activator tissue type), and ITGB8 (integrin beta 8). To determine if the regulation could be directly affected by the GATA5 levels we examined if GATA binding elements (WGATAR) were present in their promoters. Most of the genes examined possessed GATA elements in their promoters. We also examined the presence of other regulatory elements known to bind transcription factors involved in the regulation of inflammation or extracellular matrix, such as NFKB, NFAT, STAT, and SMAD which transduce the nuclear response to various cytokines and extracellular signals[122–125]. Additionally, GATA proteins were shown to act synergistically with most of these transcription factors. For example, GATA5 was shown to act cooperatively with NFAT in endothelial cells[53]. Other GATA proteins were shown to cooperate with STATs, SMADs, and NF-κB[126–131]. Interestingly, we found that several genes contained clusters of these sites in proximity to GATA sites. GATA sites in the clusters analyzed have a trend to be near NFAT and STAT, as shown for on anti-inflammatory genes (NQO2, IGFBP1) and on tight junction genes (OCLN, PRKACB, PRKAR2B) (Figure 24). The proximity of the NFAT and STAT sites suggest their interaction with GATA could be required for transcriptional activation of target genes.

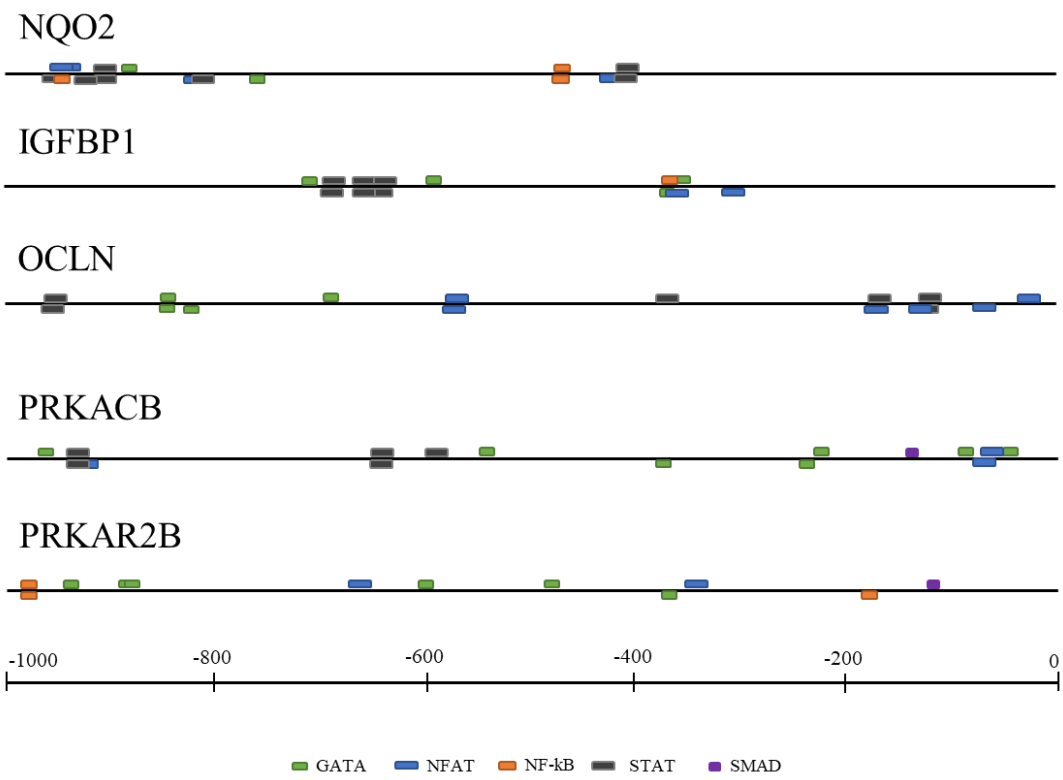

Figure 24. GATA, NF-kB, STAT, SMAD and NFAT binding site location on promoter of genes (-1000bp)

Gene expression was also evaluated in newly generated HDMEC with GATA5 overexpression. In the overexpressing cells the transcript level of only two of the inflammatory genes tested was changed: BIRC5 and myosin light chain 9 (MYL9). Several other inflammatory genes such as ICAM1, ITGB8, and IL-6 expression showed trends toward being decreased but the changes did not reach statistical significance. With respect to cellular adhesion genes, the expression of CLDN1 was decreased while the expression of TJP1 did not change. The transcript levels of E and P-selectin were measured in both knockdown and overexpression cell lines. mRNA levels were not changed in either condition, indicating that GATA5 does not regulate selectins gene transcription.

The effect of GATA5 was evaluated at the basal, unstimulated state but also in the response to TNFα. At the basal state, we found that the expression of ITGB8, ABCA1, and PLAT is highly increased as a result of the loss of GATA5 expression. Several tight junction gene expressions are altered following changes in the level of GATA5. Most notably the expression of CLDN1 and TJP1 are highly downregulated. We did not observe any change in the expression of ICAM1 in response to changes of GATA5 levels. The changes observed in the gene expression of GATA5 KD cells indicate a role for GATA5 in the regulation of the inflammatory response and in cellular adhesion. We next evaluated if the altered levels of GATA5 in endothelial cells would affect the response to a TNFα treatment. The expression of ICAM1 was not altered after the TNFα treatment. It has been shown that the expression of ICAM1 is increased after treatment with TNFα however, its expression was measured 24h after the treatment[132]. We measured the gene levels 3h after the treatment the expression of ICAM1 may not have increased in this shorter time period. Once treated with TNFα the endothelial cells with an altered level of GATA5 show lower levels of tight junction related transcripts (OCLN and CLDN1). This could indicate a weakness in the cellular junctions, which would result in an increase in vessel permeability. The transcript levels of cellular adhesion genes (ITGB8 and E-selectin) are also differentially regulated as a result of the lower levels of GATA5. The expression of E-selectin is not as stimulated in the GATA5 modified HDMECs once treated with TNFα. This could be a result of compensation for the increase in the expression of integrins such as ITGB8. The increase in cellular adhesion combined with the weaker cellular junctions would allow for an increase in immune cell migration.

The majority of mice inflammatory models have been found to act through different mechanisms than the ones found in humans and are therefore ineffective to screen potential new

anti-inflammatory drugs[133]. To evaluate if the deletion of Gata5 in mice had the same effect as the one observed in the human endothelial knockdown cells, we isolated the endothelial cells from the mice's lungs. Lung endothelial cells were selected as they are involved in several various inflammatory diseases, including COPD[134]. Their isolation is well established and is commonly used in the evaluation of inflammatory processes[103,135]. In the mice, the expression level of the inflammatory gene clusterin (Clu) were significantly upregulated while the expression of myosin light chain 9 (Myl9) was significantly decreased. Several genes trend towards being significantly downregulated including myosin light chain kinase (Mylk) and the selectins (E and P). Other genes like Plat and ATP-binding cassette, subfamily A, member 1 (Abca1) have a trend to be upregulated. No other changes were noted among cellular adhesion genes. As these are lung endothelial cells, they may have a different response than those found in other endothelial beds. Among other, it is possible that other endothelial expressed GATA factors such as GATA2, GATA4 and GATA6 may regulate GATA5-dependent genes in the same or opposite direction. Since these factors are differentially expressed in various endothelial cells (previous work from our group as well as other publications and our unpublished results), they could affect GATA5 dependent genes differently in different endothelial cells[54,136,137]. These endothelial cells were primary culture of female mice while our HDMECs are established cell culture lines from a male patient. Furthermore, female endothelial cells have been shown to have different physical and molecular responses compared to males in microvasculature[138]. In the future, the consequence of loss of GATA5 on gene expression in other endothelial cell beds, such as those from the heart and aorta should be evaluated.

The interaction between GATA5 and inflammatory genes has not been established. The only previously shown interaction in the literature between GATA5 and an inflammatory gene involves IL-6 in biliary epithelial cells. It was shown that once treated with IL-6 the human intrahepatic biliary endothelial cells downregulated their expression of GATA5[139]. We report the first evidence that GATA5 may regulate the transcription of several endothelial genes involved in the inflammatory response including IL-6, BIRC5, CLDN1, MYL-9, MYH10, ITGB8, OCLN, TJP1.

Finally, as our compounds were designed to block the selectin interactions, we examined the effects of the loss of GATA5 on the selectins. The basal mRNA level of both E and P-selectin were not altered by the loss or increased expression of GATA5 in the HDMECs. Once the knockdown cells were treated with TNFα only the expression of E-selectin was increased as indicated in the literature[106]. This suggested that the loss of GATA5 did not play a role in the transcriptional regulation of the selectins and possibly their ability to recruit leukocytes. To confirm this, we performed a cell-cell adhesion assay using non-stimulated HDMECs. There was no increase in the immune cell recruitment to the GATA5 knockdown endothelial cells under basal, non-stimulated conditions. Our combined results suggest that GATA5 could regulate the expression levels of tight junction and anti-inflammatory genes. Reduced levels of GATA5 in endothelial vascular cells would lead to an increased vascular permeability, leading to an increase of migrating immune cells.

Understanding the mechanisms of the inflammatory response will allow the identification of novel targets for the development of new anti-inflammatories. The importance of the development of new anti-inflammatory treatments has been underscored in the recent crisis of SARS-CoV-2 (COVID-19). Patients infected with COVID-19 are susceptible to develop acute respiratory distress syndrome (ARDS) which can have life-long consequences. Once exposed to the virus, lung alveoli cells increase their expression of cytokine signaling leading to the activation of the endothelial cells[140]. The excessive release of cytokines, also known as cytokine storm, is thought to be one of the major causes of ARDS. This stimulates excessive recruitment of neutrophils and monocytes causing injury[141]. The results from my research project show that some of our new anti-inflammatory molecules are able to reduce the amount of neutrophil migration, making them an interesting candidate for future treatment of ARDS.

References

1. Chen, L. *et al.* Inflammatory responses and inflammation-associated diseases in organs. *Oncotarget* **9**, (2018).
2. Owen, J., Punt, J. & Stranford, S. *Immunologie - 7e édition: Le cours de Janis Kuby avec questions de révision*. (Dunod, 2014).
3. Information, N. C. for B., Pike, U. S. N. L. of M. 8600 R., MD, B. & Usa, 20894. *The innate and adaptive immune systems*. (Institute for Quality and Efficiency in Health Care (IQWiG), 2016).
4. Ito, T. PAMPs and DAMPs as triggers for DIC. *J Intensive Care* **2**, (2014).
5. Aderem, A. & Underhill, D. M. MECHANISMS OF PHAGOCYTOSIS IN MACROPHAGES. *Annu. Rev. Immunol.* **17**, 593–623 (1999).
6. Rosales, C. & Uribe-Querol, E. Phagocytosis: A Fundamental Process in Immunity. *BioMed Research International* **2017**, 1–18 (2017).
7. Cooper, G. M. Lysosomes. *The Cell: A Molecular Approach. 2nd edition* (2000).
8. Topham, N. J. & Hewitt, E. W. Natural killer cell cytotoxicity: how do they pull the trigger? *Immunology* **128**, 7–15 (2009).
9. Reefman, E. *et al.* Cytokine Secretion Is Distinct from Secretion of Cytotoxic Granules in NK Cells. *The Journal of Immunology* **184**, 4852–4862 (2010).
10. Zhang, J.-M. & An, J. Cytokines, Inflammation, and Pain: *International Anesthesiology Clinics* **45**, 27–37 (2007).
11. Diaz, J. A. *et al.* P-Selectin Inhibition Therapeutically Promotes Thrombus Resolution and Prevents Vein Wall Fibrosis Better Than Enoxaparin and an Inhibitor to von Willebrand Factor. *Arterioscler Thromb Vasc Biol.* **35**, 829–837 (2015).
12. Kearon, C. Natural History of Venous Thromboembolism. *Circulation* **107**, 22I--30 (2003).

13. Stone, J. *et al.* Deep vein thrombosis: pathogenesis, diagnosis, and medical management. *Cardiovasc. Diagn. Ther.* **7**, S276–S284 (2017).
14. Galanaud, J.-P. & Kahn, S. R. Postthrombotic syndrome: a 2014 update. *Current Opinion in Cardiology* **29**, (2014).
15. Kawecki, C., Lenting, P. J. & Denis, C. V. von Willebrand factor and inflammation. *Journal of Thrombosis and Haemostasis* **15**, 1285–1294 (2017).
16. Gregor, M. F. & Hotamisligil, G. S. Inflammatory Mechanisms in Obesity. *Annu. Rev. Immunol.* **29**, 415–445 (2011).
17. Roh, J. S. & Sohn, D. H. Damage-Associated Molecular Patterns in Inflammatory Diseases. *Immune Netw* **18**, e27 (2018).
18. Maslanik, T. *et al.* The inflammasome and danger associated molecular patterns (DAMPs) are implicated in cytokine and chemokine responses following stressor exposure. *Brain, Behavior, and Immunity* **28**, 54–62 (2013).
19. Savoia, C. & Schiffrin, E. L. Inflammation in hypertension. *Current Opinion in Internal Medicine* **5**, 245–251 (2006).
20. Coussens, L. M. & Werb, Z. Inflammation and cancer. *Nature* **420**, 860–867 (2002).
21. Laine, L. Approaches to nonsteroidal anti-inflammatory drug use in the high-risk patient. *Gastroenterology* **120**, 594–606 (2001).
22. Schnitzer, T. J. Update of ACR Guidelines for Osteoarthritis: Role of the Coxibs. *Journal of Pain and Symptom Management* **23**, S24–S30 (2002).
23. Harizi, H., Corcuff, J.-B. & Gualde, N. Arachidonic-acid-derived eicosanoids: roles in biology and immunopathology. *Trends in Molecular Medicine* **14**, 461–469 (2008).
24. Schafer, A. I. Effects of Nonsteroidal Antiinflammatory Drugs on Platelet Function and Systemic Hemostasis. *The Journal of Clinical Pharmacology* **35**, 209–219 (1995).

25. Langman, M. J. S. *et al.* Risks of bleeding peptic ulcer associated with individual non-steroidal anti-inflammatory drugs. *The Lancet* **343**, 1075–1078 (1994).
26. García Rodríguez, L. A. & Jick, H. Risk of upper gastrointestinal bleeding and perforation associated with individual non-steroidal anti-inflammatory drugs. *Lancet* **343**, 769–772 (1994).
27. Gabriel, S. E., Jaakkimainen, L. & Bombardier, C. Risk for Serious Gastrointestinal Complications Related to Use of Nonsteroidal Anti-inflammatory Drugs: A Meta-analysis. *Annals of Internal Medicine* **115**, 787–796 (1991).
28. Lenzer, J. FDA advisers warn: COX 2 inhibitors increase risk of heart attack and stroke. *BMJ* **330**, 440 (2005).
29. Barnes, P. J. Anti-inflammatory Actions of Glucocorticoids: Molecular Mechanisms. *Clinical Science* **94**, 557–572 (1998).
30. Hall, S. E. *et al.* Lung type II cell and macrophage annexin I release: differential effects of two glucocorticoids. *American Journal of Physiology-Lung Cellular and Molecular Physiology* **276**, L114–L121 (1999).
31. Greaves, M. W. Anti-inflammatory action of corticosteroids. *Postgrad Med J* **52**, 631–633 (1976).
32. Barnes, P. J., Ito, K. & Adcock, I. M. Corticosteroid resistance in chronic obstructive pulmonary disease: inactivation of histone deacetylase. *The Lancet* **363**, 731–733 (2004).
33. Buchman, A. Side Effects of Corticosteroid Therapy. *Journal of Clinical Gastroenterology* **33**, 289–294 (2001).
34. Cushing, H. The Basophil Adenomas of the Pituitary Body and Their Clinical Manifestations (Pituitary Basophilism)1. *Obesity Research* **2**, 486–508 (1994).
35. Allen, D. B., Julius, J. R. & Breen, T. J. Treatment of Glucocorticoid-Induced Growth Suppression with Growth Hormone. **83**, 6 (1998).
36. Claesson-Welsh, L. Vascular permeability--the essentials. *Ups J Med Sci* **120**, 135–143 (2015).

37. Crola Da Silva, C. *et al.* Selective human endothelial cell activation by chemokines as a guide to cell homing. *Immunology* **126**, 394–404 (2009).

38. Brown, M. D., Wick, T. M. & Eckman, J. R. Activation of vascular endothelial cell adhesion molecule expression by sickle blood cells. *Pediatr Pathol Mol Med* **20**, 47–72 (2001).

39. Mantovani, A. & Dejana, E. Endothelium. in *Encyclopedia of Immunology (Second Edition)* (ed. Delves, P. J.) 802–806 (Elsevier, 1998). doi:10.1006/rwei.1999.0212.

40. Lawrence, M. B., Kansas, G. S., Kunkel, E. J. & Ley, K. Threshold Levels of Fluid Shear Promote Leukocyte Adhesion through Selectins (CD62L,P,E). *The Journal of Cell Biology* **136**, 717–727 (1997).

41. Springer, T. A. Structural basis for selectin mechanochemistry. *Proceedings of the National Academy of Sciences* **106**, 91–96 (2009).

42. Pereverzev, Y. V., Prezhdo, O. V., Forero, M., Sokurenko, E. V. & Thomas, W. E. The Two-Pathway Model for the Catch-Slip Transition in Biological Adhesion. *Biophysical Journal* **89**, 1446–1454 (2005).

43. Leick, M., Azcutia, V., Newton, G. & Luscinskas, F. W. Leukocyte recruitment in inflammation: basic concepts and new mechanistic insights based on new models and microscopic imaging technologies. *Cell Tissue Res* **355**, 647–656 (2014).

44. McEver, R. P. Selectins: initiators of leucocyte adhesion and signalling at the vascular wall. *Cardiovasc Res* **107**, 331–339 (2015).

45. Springer, T. A. & Dustin, M. L. Integrin inside-out signaling and the immunological synapse. *Current Opinion in Cell Biology* **24**, 107–115 (2012).

46. Langer, H. F. & Chavakis, T. Leukocyte - endothelial interactions in inflammation. *Journal of Cellular and Molecular Medicine* **13**, 1211–1220 (2009).

47. Tang, J.-R. *et al.* The NF-κB inhibitory proteins IκBα and IκBβ mediate disparate responses to inflammation in fetal pulmonary endothelial cells. *J Immunol* **190**, 2913–2923 (2013).

48. Rajendran, P. *et al.* The Vascular Endothelium and Human Diseases. *Int. J. Biol. Sci.* **9**, 1057–1069 (2013).

49. Kanki, Y. *et al.* Epigenetically coordinated GATA2 binding is necessary for endothelium-specific *endomucin* expression: GATA2-mediated gene regulations in endothelium. *The EMBO Journal* **30**, 2582–2595 (2011).

50. Morrisey, E. E., Ip, H. S., Tang, Z., Lu, M. M. & Parmacek, M. S. GATA-5: A Transcriptional Activator Expressed in a Novel Temporally and Spatially-Restricted Pattern during Embryonic Development. *Developmental Biology* **183**, 21–36 (1997).

51. Whitcomb, J., Gharibeh, L. & Nemer, M. From embryogenesis to adulthood: Critical role for GATA factors in heart development and function. *IUBMB Life* **72**, 53–67 (2020).

52. Song, H. *et al.* Critical Role for GATA3 in Mediating Tie2 Expression and Function in Large Vessel Endothelial Cells. *J. Biol. Chem.* **284**, 29109–29124 (2009).

53. Nemer, G. & Nemer, M. Cooperative interaction between GATA5 and NF-ATc regulates endothelial-endocardial differentiation of cardiogenic cells. *Development* **129**, 4045–4055 (2002).

54. Laforest, B., Andelfinger, G. & Nemer, M. Loss of Gata5 in mice leads to bicuspid aortic valve. *J. Clin. Invest.* **121**, 2876–2887 (2011).

55. Messaoudi, S. *et al.* Endothelial Gata5 transcription factor regulates blood pressure. *Nature Communications* **6**, 8835 (2015).

56. Jeon, S.-M., Chandel, N. S. & Hay, N. AMPK regulates NADPH homeostasis to promote tumour cell survival during energy stress. *Nature* **485**, 661 (2012).

57. Savchenko, V. L. Regulation of NADPH Oxidase Gene Expression with PKA and Cytokine IL-4 in Neurons and Microglia. *Neurotox Res* **23**, 201–213 (2013).

58. Granger, D. N. & Senchenkova, E. *Leukocyte–Endothelial Cell Adhesion*. (Morgan & Claypool Life Sciences, 2010).

59. Cummings, R. D. & Smith, D. F. The selectin family of carbohydrate-binding proteins: Structure and importance of carbohydrate ligands for cell adhesion. *BioEssays* **14**, 849–856 (1992).

60. Tedder, T. F., Steeber, D. A., Chen, A. & Engel, P. The selectins: vascular adhesion molecules. *The FASEB Journal* **9**, 866–873 (1995).

61. Graczyk, M. *et al.* Role of E-selectin and platelet endothelial cell adhesion molecule 1 in gastritis in food allergy patients. *Postepy Dermatol Alergol* **30**, 271–276 (2013).

62. Gotsch, U., Jäger, U., Dominis, M. & Vestweber, D. Expression of P-selectin on endothelial cells is upregulated by LPS and TNF-alpha in vivo. *Cell Adhes. Commun.* **2**, 7–14 (1994).

63. Hirata, T., Furie, B. C. & Furie, B. P-, E-, and L-Selectin Mediate Migration of Activated CD8 $^{+}$ T Lymphocytes into Inflamed Skin. *J Immunol* **169**, 4307–4313 (2002).

64. Valentijn, K. M., Sadler, J. E., Valentijn, J. A., Voorberg, J. & Eikenboom, J. Functional architecture of Weibel-Palade bodies. *Blood* **117**, 5033–5043 (2011).

65. Barthel, S. R., Gavino, J. D., Descheny, L. & Dimitroff, C. J. Targeting selectins and selectin ligands in inflammation and cancer. *Expert Opin Ther Targets* **11**, 1473–1491 (2007).

66. Hidalgo, A., Peired, A. J., Wild, M., Vestweber, D. & Frenette, P. S. Complete identification of E-selectin ligand activity on neutrophils reveals a dynamic interplay and distinct functions of PSGL-1, ESL-1 and CD44. *Immunity* **26**, 477–489 (2007).

67. Cummings, R. D. Structure and function of the selectin ligand PSGL-1. *Braz. J. Med. Biol. Res.* **32**, 519–528 (1999).

68. Hirose, M., Kawashima, H. & Miyasaka, M. A functional epitope on P-selectin that supports binding of P-selectin to P-selectin glycoprotein ligand-1 but not to sialyl Lewis X oligosaccharides. *Int Immunol* **10**, 639–649 (1998).

69. Fukuda, M., Hiraoka, N. & Yeh, J.-C. C-Type Lectins and Sialyl Lewis X Oligosaccharides. *J Cell Biol* **147**, 467–470 (1999).

70. Somers, W. S., Tang, J., Shaw, G. D. & Camphausen, R. T. Insights into the Molecular Basis of Leukocyte Tethering and Rolling Revealed by Structures of P- and E-Selectin Bound to SLeX and PSGL-1. *Cell* **103**, 467–479 (2000).

71. Burley, S. K. *et al.* RCSB Protein Data Bank: biological macromolecular structures enabling research and education in fundamental biology, biomedicine, biotechnology and energy. *Nucleic Acids Research* **47**, D464–D474 (2019).

72. Sehnal, D., Rose, A., Koca, J., Burley, S. & Velankar, S. Mol*: Towards a Common Library and Tools for Web Molecular Graphics. *Workshop on Molecular Graphics and Visual Analysis of Molecular Data* 5 pages (2018) doi:10.2312/MOLVA.20181103.

73. Blann, A. The adhesion molecule P-selectin and cardiovascular disease. *European Heart Journal* **24**, 2166–2179 (2003).

74. Ley, K. The role of selectins in inflammation and disease. *Trends in Molecular Medicine* **9**, 263–268 (2003).

75. Canalli, A. A. *et al.* Participation of Mac-1, LFA-1 and VLA-4 integrins in the in vitro adhesion of sickle cell disease neutrophils to endothelial layers, and reversal of adhesion by simvastatin. *Haematologica* **96**, 526–533 (2011).

76. Läubli, H. & Borsig, L. Selectins promote tumor metastasis. *Seminars in Cancer Biology* **20**, 169–177 (2010).

77. Bennewitz, M. F. *et al.* P-selectin–deficient mice to study pathophysiology of sickle cell disease. *Blood Advances* **4**, 266–273 (2020).

78. Pace, B. S., Ofori-Acquah, S. F. & Peterson, K. R. Sickle cell disease: genetics, cellular and molecular mechanisms, and therapies. *Anemia* **2012**, 143594–143594 (2012).

79. Darrow, M. C. *et al.* Visualizing red blood cell sickling and the effects of inhibition of sphingosine kinase 1 using soft X-ray tomography. *J Cell Sci* **129**, 3511–3517 (2016).

80. Wood, K., Russell, J., Hebbel, R. P. & Granger, D. N. Differential Expression of E- and P-Selectin in the Microvasculature of Sickle Cell Transgenic Mice. *Microcirculation* **11**, 377–385 (2004).

81. Okpala, I. Leukocyte adhesion and the pathophysiology of sickle cell disease. *Current Opinion in Hematology* **13**, 40–44 (2006).

82. Seyfried, T. N. & Huysentruyt, L. C. On the origin of cancer metastasis. *Crit Rev Oncog* **18**, 43–73 (2013).

83. Pinho, S. S. & Reis, C. A. Glycosylation in cancer: mechanisms and clinical implications. *Nat Rev Cancer* **15**, 540–555 (2015).

84. Häuselmann, I. & Borsig, L. Altered Tumor-Cell Glycosylation Promotes Metastasis. *Front. Oncol.* **4**, (2014).

85. Häuselmann, I. *et al.* Monocyte Induction of E-Selectin–Mediated Endothelial Activation Releases VE-Cadherin Junctions to Promote Tumor Cell Extravasation in the Metastasis Cascade. *Cancer Res* **76**, 5302–5312 (2016).

86. Wessel, F. *et al.* Leukocyte extravasation and vascular permeability are each controlled in vivo by different tyrosine residues of VE-cadherin. *Nat Immunol* **15**, 223–230 (2014).

87. Chames, P., Van Regenmortel, M., Weiss, E. & Baty, D. Therapeutic antibodies: successes, limitations and hopes for the future. *Br J Pharmacol* **157**, 220–233 (2009).

88. Ataga, K. I. *et al.* Crizanlizumab for the Prevention of Pain Crises in Sickle Cell Disease. *N Engl J Med* **376**, 429–439 (2017).

89. Compain, P. Glycomimetics: Design, Synthesis, and Therapeutic Applications. *Molecules* **23**, 1658 (2018).

90. Reina, J. J. & Bernardi, A. Carbohydrate mimics and lectins: a source of new drugs and therapeutic opportunities. *Mini Rev Med Chem* **12**, 1434–1442 (2012).

91. Chang, J. *et al.* GMI-1070, a novel pan-selectin antagonist, reverses acute vascular occlusions in sickle cell mice. *Blood* **116**, 1779–1786 (2010).

92. Palma-Vargas, J. M. *et al.* Small-molecule selectin inhibitor protects against liver inflammatory response after ischemia and reperfusion. *Journal of the American College of Surgeons* **185**, 365–372 (1997).

93. Kogan, T. P. *et al.* Novel Synthetic Inhibitors of Selectin-Mediated Cell Adhesion: Synthesis of 1,6-Bis[3-(3-carboxymethylphenyl)-4-(2-α-d-mannopyranosyloxy)phenyl]hexane (TBC1269). *J. Med. Chem.* **41**, 1099–1111 (1998).

94. Hicks, A. E. R. *et al.* The anti-inflammatory effects of a selectin ligand mimetic, TBC-1269, are not a result of competitive inhibition of leukocyte rolling in vivo. *Journal of Leukocyte Biology* **77**, 59–66 (2005).

95. Avila, P. C. *et al.* Effect of a single dose of the selectin inhibitor TBC1269 on early and late asthmatic responses. *Clinical & Experimental Allergy* **34**, 77–84 (2004).

96. Meyer, M., Jilma, B., Zahlten, R. & Wolff, G. Physiochemical properties, safety and pharmacokinetics of Bimosiamose disodium after intravenous administration. *International journal of clinical pharmacology and therapeutics* **43**, 463–71 (2005).

97. Smith, A. Rivipansel flunks Phase III sickle cell trial. *PharmaTimes* http://www.pharmatimes.com/news/rivipansel_flunks_phase_iii_sickle_cell_trial_1296433 (2019).

98. Calosso, M. *et al.* Acyclic tethers mimicking subunits of polysaccharide ligands: selectin antagonists. *ACS Med Chem Lett* **5**, 1054–1059 (2014).

99. Schindelin, J. *et al.* Fiji: an open-source platform for biological-image analysis. *Nat Methods* **9**, 676–682 (2012).

100. Ray, A. & Dittel, B. N. Isolation of Mouse Peritoneal Cavity Cells. *JoVE* 1488 (2010) doi:10.3791/1488.

101. Debrus, S. *et al.* The Zinc Finger-Only Protein Zfp260 Is a Novel Cardiac Regulator and a Nuclear Effector of 1-Adrenergic Signaling. *Molecular and Cellular Biology* **25**, 8669–8682 (2005).

102. Kopec, A. M., Rivera, P. D., Lacagnina, M. J., Hanamsagar, R. & Bilbo, S. D. Optimized solubilization of TRIzol-precipitated protein permits Western blotting analysis to maximize data available from brain tissue. *Journal of Neuroscience Methods* **280**, 64–76 (2017).

103. Pang, H. Isolation of Endothelial Cells from Mice. *Bio-protocol* **2**, e205 (2012).

104. Nguyen, L. A., He, H. & Pham-Huy, C. Chiral drugs: an overview. *Int J Biomed Sci* **2**, 85–100 (2006).

105. Xue, J. *et al.* NF-κB regulates thrombin-induced ICAM-1 gene expression in cooperation with NFAT by binding to the intronic NF-κB site in the ICAM-1 gene. *Physiol Genomics* **38**, 42–53 (2009).

106. Rahman, A., Kefer, J., Bando, M., Niles, W. D. & Malik, A. B. E-selectin expression in human endothelial cells by TNF-α-induced oxidant generation and NF-κB activation. *American Journal of Physiology-Lung Cellular and Molecular Physiology* **275**, L533–L544 (1998).

107. Hermida, M. D. R., Malta, R., de S. Santos, M. D. P. C. & dos-Santos, W. L. C. Selecting the right gate to identify relevant cells for your assay: a study of thioglycollate-elicited peritoneal exudate cells in mice. *BMC Res Notes* **10**, 695 (2017).

108. Mizgerd, J. P. *et al.* Neutrophil Emigration in the Skin, Lungs, and Peritoneum: Different Requirements for CD11/CD18 Revealed by CD18-deficient Mice. *J Exp Med* **186**, 1357–1364 (1997).

109. Bosse, R. & Vestweber, D. Only simultaneous blocking of the L- and P-selectin completely inhibits neutrophil migration into mouse peritoneum. *European Journal of Immunology* **24**, 3019–3024 (1994).

110. Krämer, A., Green, J., Pollard, J. & Tugendreich, S. Causal analysis approaches in Ingenuity Pathway Analysis. *Bioinformatics* **30**, 523–530 (2014).

111. Cartharius, K. *et al.* MatInspector and beyond: promoter analysis based on transcription factor binding sites. *Bioinformatics* **21**, 2933–2942 (2005).

112. Ju, L. *et al.* Enhanced expression of Survivin has distinct roles in adipocyte homeostasis. *Cell Death Dis* **8**, e2533–e2533 (2018).

113. Hoevel, T., Macek, R., Mundigl, O., Swisshelm, K. & Kubbies, M. Expression and targeting of the tight junction protein CLDN1 in CLDN1-negative human breast tumor cells. *Journal of Cellular Physiology* **191**, 60–68 (2002).

114. Weber, C. R., Nalle, S. C., Tretiakova, M., Rubin, D. T. & Turner, J. R. Claudin-1 and claudin-2 expression are elevated in inflammatory bowel disease and may contribute to early neoplastic transformation. *Lab Invest* **88**, 1110–1120 (2008).

115. Kimura, M. Y., Koyama-Nasu, R., Yagi, R. & Nakayama, T. A new therapeutic target: the CD69-Myl9 system in immune responses. *Semin Immunopathol* **41**, 349–358 (2019).

116. Kim, H.-T. *et al.* Myh10 deficiency leads to defective extracellular matrix remodeling and pulmonary disease. *Nat Commun* **9**, 4600 (2018).

117. Falgarone, G. & Chiocchia, G. Chapter 8 Clusterin: A Multifacet Protein at the Crossroad of Inflammation and Autoimmunity. in *Advances in Cancer Research* vol. 104 139–170 (Academic Press, 2009).

118. Lee, C.-W. *et al.* Transcriptional regulation of VCAM-1 expression by tumor necrosis factor-α in human tracheal smooth muscle cells: Involvement of MAPKs, NF-κB, p300, and histone acetylation. *Journal of Cellular Physiology* **207**, 174–186 (2006).

119. Rennard, S. I. *et al.* The Safety and Efficacy of Infliximab in Moderate to Severe Chronic Obstructive Pulmonary Disease. *Am J Respir Crit Care Med* **175**, 926–934 (2007).

120. Wong, R. S. Y. *et al.* Comparison of the Potential Multiple Binding Modes of Bicyclam, Monocylam, and Noncyclam Small-Molecule CXC Chemokine Receptor 4 Inhibitors. *Mol Pharmacol* **74**, 1485–1495 (2008).

121. Murdoch, C. CXCR4: chemokine receptor extraordinaire. *Immunological Reviews* **177**, 175–184 (2000).

122. Deshpande, R., Khalili, H., Pergolizzi, R. G., Michael, S. D. & Chang, M.-D. Y. Estradiol Down-Regulates LPS-Induced Cytokine Production and NFkB Activation in Murine Macrophages. *American Journal of Reproductive Immunology* **38**, 46–54 (1997).

123. Fric, J. *et al.* NFAT control of innate immunity. *Blood* **120**, 1380–1389 (2012).

124. Guo, L. *et al.* IL-1 family members and STAT activators induce cytokine production by Th2, Th17, and Th1 cells. *Proceedings of the National Academy of Sciences* **106**, 13463–13468 (2009).

125. Yoshimura, A., Wakabayashi, Y. & Mori, T. Cellular and molecular basis for the regulation of inflammation by TGF-. *Journal of Biochemistry* **147**, 781–792 (2010).

126. Rysä, J. *et al.* GATA-4 Is an Angiogenic Survival Factor of the Infarcted Heart. *Circ Heart Fail* **3**, 440–450 (2010).

127. Wang, J. *et al.* Convergence of Protein Kinase C and JAK-STAT Signaling on Transcription Factor GATA-4. *Mol Cell Biol* **25**, 9829–9844 (2005).

128. Benchabane, H. & Wrana, J. L. GATA- and Smad1-Dependent Enhancers in the Smad7 Gene Differentially Interpret Bone Morphogenetic Protein Concentrations. *Mol Cell Biol* **23**, 6646–6661 (2003).

129. Blokzijl, A. Physical and Functional Interaction between GATA-3 and Smad3 Allows TGF-☒ Regulation of GATA Target Genes. *Current Biology* 11.

130. Thangavel, C. *et al.* NF-κB and GATA-Binding Factor 6 Repress Transcription of Caveolins in Bladder Smooth Muscle Hypertrophy. *The American Journal of Pathology* **189**, 847–867 (2019).

131. Chen, G.-Y., Sakuma, K. & Kannagi, R. Significance of NF-κB/GATA Axis in Tumor Necrosis Factor-α-induced Expression of 6-Sulfated Cell Recognition Glycans in Human T-lymphocytes. *J Biol Chem* **283**, 34563–34570 (2008).

132. Burke-Gaffney, A. & Hellewell, P. G. Tumour necrosis factor-α-induced ICAM-1 expression in human vascular endothelial and lung epithelial cells: modulation by tyrosine kinase inhibitors. *British Journal of Pharmacology* **119**, 1149–1158 (1996).

133. Of men, not mice. *Nat Med* **19**, 379–379 (2013).

134. Chambers, E., Rounds, S. & Lu, Q. Pulmonary Endothelial Cell Apoptosis in Emphysema and Acute Lung Injury. *Adv Anat Embryol Cell Biol* **228**, 63–86 (2018).

135. Sievert, W. *et al.* Late proliferating and inflammatory effects on murine microvascular heart and lung endothelial cells after irradiation. *Radiotherapy and Oncology* **117**, 376–381 (2015).

136. Nemer, G. & Nemer, M. Transcriptional activation of BMP-4 and regulation of mammalian organogenesis by GATA-4 and -6. *Developmental Biology* **254**, 131–148 (2003).

137. Dorfman, D. M., Wilson, D. B., Bruns, G. A. & Orkin, S. H. Human transcription factor GATA-2. Evidence for regulation of preproendothelin-1 gene expression in endothelial cells. *J. Biol. Chem.* **267**, 1279–1285 (1992).

138. Huxley, V. H. & Kemp, S. S. Sex-Specific Characteristics of the Microcirculation. *Adv Exp Med Biol* **1065**, 307–328 (2018).

139. Liu, P. *et al.* Methylation-Mediated Silencing of GATA5 Gene Suppresses Cholangiocarcinoma Cell Proliferation and Metastasis. *Transl Oncol* **11**, 585–592 (2018).

140. Ye, Q., Wang, B. & Mao, J. The pathogenesis and treatment of the `Cytokine Storm' in COVID-19. *J Infect* **80**, 607–613 (2020).

141. Kim, E. S. *et al.* Clinical Progression and Cytokine Profiles of Middle East Respiratory Syndrome Coronavirus Infection. *J Korean Med Sci* **31**, 1717–1725 (2016).